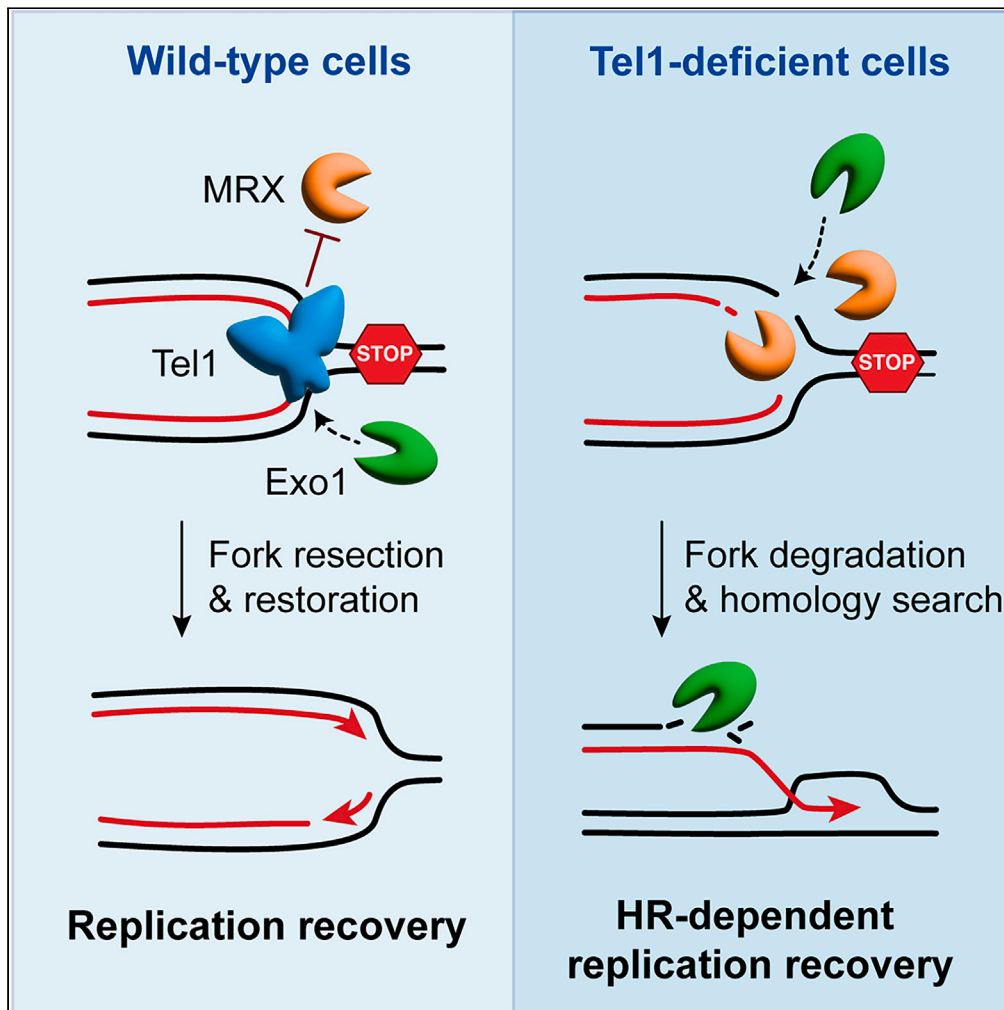**Article**

Exo1 cooperates with Tel1/ATM in promoting recombination events at DNA replication forks

Michela Galli,
Chiara Frigerio,
Chiara Vittoria
Colombo, Erika
Casari, Maria Pia
Longhese, Michela
Clerici

mariapia.longhese@unimib.it
(M.P.L.)
michela.clerici@unimib.it (M.C.)

Highlights
Exo1 supports the viability
of cells with Tel1
dysfunctions upon
replication stress

Tel1 limits replication
block-induced
recombination between
inverted DNA repeats

Exo1 is essential for the
hyper-recombination in
Tel1-deficient cells

MRX and Ku contribute to
hyper-recombination in
Tel1-deficient cells

Article

Exo1 cooperates with Tel1/ATM in promoting recombination events at DNA replication forks

Michela Galli,[1] Chiara Frigerio,[1] Chiara Vittoria Colombo,[1] Erika Casari,[1] Maria Pia Longhese,[1,*] and Michela Clerici[1,2,*]

SUMMARY

Tel1/ataxia telangiectasia mutated (ATM) kinase plays multiple functions in response to DNA damage, promoting checkpoint-mediated cell-cycle arrest and repair of broken DNA. In addition, *Saccharomyces cerevisiae* Tel1 stabilizes replication forks that arrest upon the treatment with the topoisomerase poison camptothecin (CPT). We discover that inactivation of the Exo1 nuclease exacerbates the sensitivity of Tel1-deficient cells to CPT and other agents that hamper DNA replication. Furthermore, cells lacking both Exo1 and Tel1 activities exhibit sustained checkpoint activation in the presence of CPT, indicating that Tel1 and Exo1 limit the activation of a Mec1-dependent checkpoint. The absence of Tel1 or its kinase activity enhances recombination between inverted DNA repeats induced by replication fork blockage in an Exo1-dependent manner. Thus, we propose that Exo1 processes intermediates arising at stalled forks in *tel1* mutants to promote DNA replication recovery and cell survival.

INTRODUCTION

Tel1/ataxia telangiectasia mutated (ATM) and Mec1/ATM and Rad3 related (ATR) play crucial functions in maintaining genome stability, being the master regulators of the DNA damage response (DDR). Tel1/ATM and Mec1/ATR are serine/threonine protein kinases with a head-to-head dimeric conformation, which detect aberrant DNA structures and orchestrate a complex signal transduction cascade that coordinates DNA damage repair with the progression of the cell cycle.[1–4] Once activated, Tel1/ATM and Mec1/ATR temporarily halt cell-cycle progression through the phosphorylation of the checkpoint effector kinases Rad53/CHK2 and Chk1, along with their adaptors Rad9/53BP1 and Mrc1/Claspin.[3,5,6] Mec1/ATR, together with Ddc2/ATR-interacting protein (ATRIP), recognizes long single-stranded DNA (ssDNA) stretches coated by the replication protein A (RPA) complex,[7,8] while Tel1/ATM is activated at both DNA double-strand breaks (DSBs) and protein-bound DNA ends through interaction with the MRX/MRN (Mre11-Rad50-Xrs2/NBS1) complex.[9–11]

DSBs can be repaired by either non-homologous end-joining (NHEJ), which catalyzes the direct ligation of the broken ends, or homologous recombination (HR), which uses an intact homologous chromosome as a template to repair the break.[12,13] HR is initiated by a two-step nucleolytic processing of the 5′-terminated DSB ends, a mechanism referred to as resection. The Mre11 subunit of the MRX/MRN complex, stimulated by Sae2/CtIP, incises the 5′-terminated strands at the DSB end.[14] This nick allows Mre11 to degrade DNA back toward the end through its 3′–5′ exonucleolytic activity, and concomitantly creates an entry site for the long-range resection nucleases Exo1 and Sgs1-Dna2 that degrade the same strand in the 5′-3′ direction.[15–19] The Rad51 recombinase rapidly covers the ssDNA tails generated by resection, thus stimulating the invasion of a homologous duplex and the completion of HR.[12]

Saccharomyces cerevisiae Tel1 has been initially identified because of its function in maintaining the ends of linear chromosomes in the nucleoprotein structures called telomeres.[20,21] Further evidence has shown that Tel1 supports DSB repair in the presence of hindrances by participating in the metabolism of different DSB-containing structures. Specifically, Tel1 promotes DSB repair through HR by stimulating DSB end resection and by holding the two DSB ends in close proximity.[22–26] Both these functions likely rely on a kinase-independent Tel1 function that stabilizes the MRX complex onto the DNA.[26,27] On the contrary, Tel1 kinase activity stimulates a relocation of the Ku heterodimer from the DSB ends to more internal chromosome regions.[25,28] Since Ku promotes NHEJ and simultaneously restricts access of resection nucleases to DNA ends, this Tel1-mediated Ku relocation likely contributes to HR. In addition, the persistence of histones in the surroundings of DSB ends in the absence of Tel1 kinase activity suggests that Tel1 activity may also stimulate, directly or indirectly, chromatin remodeling at DSBs.[25]

Furthermore, in both yeast and mammals, Tel1/ATM supports DNA replication in conditions that induce replication fork reversal, including the persistence of the Top1 topoisomerase onto the DNA caused by camptothecin (CPT).[29] Reversed forks result from unwinding and annealing of the nascent DNA strands, forming a four-way junction with a regressed arm.[30,31] Controlled degradation of the regressed arm by nucleases can aid replication recovery, while an excessive degradation of the nascent strand can lead to fork disassembly, uncomplete chromosome duplication, or unscheduled HR-mediated events. Therefore, both the formation and the nucleolytic processing of reversed forks

[1]Dipartimento di Biotecnologie e Bioscienze, Università degli Studi di Milano-Bicocca, Milano, Italy
[2]Lead contact
*Correspondence: mariapia.longhese@unimib.it (M.P.L.), michela.clerici@unimib.it (M.C.)
https://doi.org/10.1016/j.isci.2024.110410

must be tightly regulated to promote replication recovery.[30–32] In budding yeast, Tel1 stabilizes reversed forks in CPT-treated cells by counteracting their degradation by Mre11, and this likely contributes to replication recovery and cell survival.[33] Interestingly, Exo1 appears to be dispensable for fork degradation in the absence of Tel1,[33] while it is responsible for fork degradation both in checkpoint mutants treated with methyl methanesulfonate (MMS) or hydroxyurea (HU)[34,35] and in recombination mutants in which a protein-induced barrier arrests fork progression.[32,36,37] Besides being involved in fork processing and DSB resection, Exo1 participates in DNA mismatch repair (MMR) and crossover (CO) promotion during meiosis.[16,38,39]

In mammals, ATM promotes fork reversal together with the TIP60 acetyltransferase by recruiting the SMARCAL1 translocase to stalled replication forks.[40] Reversed forks are protected against excessive nucleolytic degradation by the BRCA tumor suppressor pathway, whose deficiencies cause extensive fork degradation by MRE11 and other nucleases.[41–43] Although TIP60 and ATM promote fork reversal by acting in the same pathway, TIP60 inactivation suppresses chemotherapy sensitivity of BRCA-deficient cells, whereas ATM inhibition exacerbates it.[40] This suggests that ATM may play additional functions at stalled replication forks.

By investigating the interplays between Tel1 and Exo1, here we discover that the lack of Exo1, or of its nuclease activity, exacerbates the sensitivity of cells lacking Tel1, or its kinase activity, to treatments with compounds that perturb DNA replication. tel1 exo1 mutant cells released in CPT in S-phase showed persistent checkpoint activation, while they are still capable to repair a DNA DSB by ectopic recombination. By using an inducible system that causes a replication block, we found that Tel1 limits recombination between inverted DNA repeats adjacent to a stalled replication fork through its kinase activity. Exo1 is strictly required for these HR-dependent events in Tel1-deficient cells, suggesting that Exo1 supports the viability of tel1 mutant cells by promoting HR-dependent events that allow fork recovery.

RESULTS

Exo1 supports the viability of cells lacking Tel1 or its kinase activity in response to DNA damage and replication stress

Cells lacking Tel1 or its kinase activity show a mild sensitivity to CPT (Figure 1A),[23,33,44] which can be due, at least in part, to a Tel1 function in protecting reversed forks from degradation.[33] While Exo1 degrades stalled forks in wild-type cells and in the absence of the intra-S checkpoint,[34,35] it does not appear to be involved in degrading the regressed arm of reversed forks in the absence of Tel1.[33] This finding does not exclude that Exo1 may contribute to other DDR pathways in the absence of Tel1.

To thoroughly investigate the interplays between Tel1 and Exo1 in the DDR, we analyzed the sensitivity to genotoxic treatments of cells carrying TEL1 deletion or the tel1-kd allele that abolishes Tel1 kinase activity,[45] either in the presence or in the absence of Exo1. Exponentially growing wild-type, tel1Δ, tel1Δ exo1Δ, tel1-kd, tel1-kd exo1Δ, and exo1Δ cell cultures were spotted out onto YEPD plates with or without different concentrations of CPT, the replication inhibitor HU or the alkylating agent MMS. While tel1Δ and tel1-kd cells exhibited reduced viability after three days of growth on plates containing 15 μM CPT, tel1Δ exo1Δ and tel1-kd exo1Δ double mutant cells lost viability even in the presence of lower CPT doses, as well as in the presence of HU or MMS (Figure 1A). Since inactivation of Tel1 or its kinase activity by itself conferred CPT sensitivity, we confirmed the synthetic growth defects in CPT due to the concomitant inactivation of Exo1 and Tel1 by quantifying the survival of wild-type, tel1Δ, tel1Δ exo1Δ, and exo1Δ cell cultures spread onto YEPD plates containing increasing CPT concentrations. After three days of growth onto 6–9 μM CPT-containing plates at 25°C, tel1Δ exo1Δ cells exhibited an increased viability loss compared to tel1Δ and exo1Δ cells, which formed colonies as wild-type cells (Figure 1B). Conversely, tel1Δ and exo1Δ cells lost viability starting from 12 μM CPT, where tel1Δ exo1Δ cells were unable to form colonies (Figure 1B). Similar results were obtained with tel1-kd and tel1-kd exo1Δ cell cultures (Figure S1A).

Interestingly, Exo1 and Tel1 inactivation did not cause synthetic growth defects after UV irradiation. In fact, wild-type, tel1Δ, tel1-kd, tel1Δ exo1Δ, tel1-kd exo1Δ, and exo1Δ cells lost viability to similar extents when they were exposed to different UV doses (Figures 1C and S1B). CPT, MMS, and HU mainly exert their toxicity during DNA replication, while UV light, which was administered as an acute treatment to asynchronous cell cultures, likely induces lesions that are detected and repaired outside of the S-phase. In addition, UV-induced DNA lesions are known to slow down but not to stop DNA replication, thanks to the existence of DNA lesion tolerance and lesion bypass pathways that allow the replication fork to pass over the lesion or to restart DNA replication downstream to damaged site.[46–48]

We hypothesized that Exo1 supports Tel1 functions specifically in the context of DNA replication stress. To assess this possibility, we exposed wild-type, tel1Δ, exo1Δ, and tel1Δ exo1Δ cells to acute or chronic treatment with the radiomimetic drug phleomycin (phleo), which is thought to generate single-strand breaks and DSBs that are sensed by the DDR in any cell-cycle phase.[49] For the acute treatment, we added high concentrations of phleo for 2 h to cells arrested in G2 with nocodazole, followed by the evaluation of cell survival on YEPD plates (Figure 1D). For chronic exposure, we determined the viability of cells spread onto YEPD plates containing different phleo concentrations (Figure 1E). sae2Δ cells were used as a control since they lose viability after both acute and chronic treatments with phleo (Figures 1D and 1E).[27] The acute treatments with phleo in G2 slightly reduced cell viability of wild-type, tel1Δ, exo1Δ, and tel1Δ exo1Δ cells to similar extents (Figure 1D). Conversely, tel1Δ exo1Δ cells displayed an increased sensitivity to chronic phleo exposure compared to both tel1Δ and exo1Δ cells (Figure 1E). Similarly, tel1-kd exo1Δ cells were more sensitive than tel1-kd and exo1Δ cells to chronic treatments with phleo, while they lost viability as tel1-kd and exo1Δ cells after acute treatments (Figures S1C and S1D). These results suggest that the lack of Exo1 exacerbates the sensitivity of cells lacking Tel1 or its kinase activity to genotoxic treatments that interfere with DNA replication.

Most, if not all, of the functions carried out by Exo1 during a mitotic cell cycle require its nuclease activity.[50] To investigate whether the nuclease activity of Exo1 is necessary to support the viability of tel1 mutants, we transformed wild-type, tel1Δ, and tel1Δ exo1Δ cells with plasmids carrying a wild-type EXO1 gene or the exo1-D171A allele, which encodes a nuclease-defective Exo1 variant.[51] Expression of
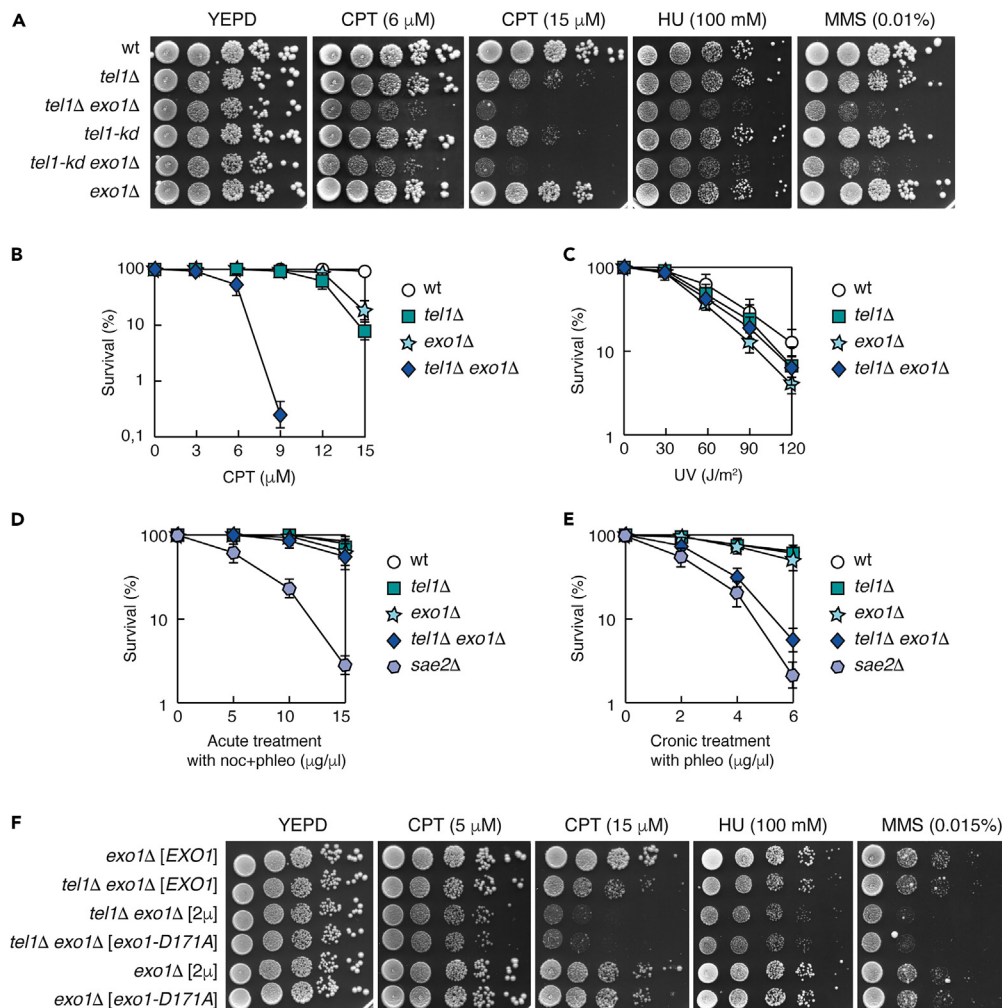
Figure 1. The lack of Exo1 exacerbates the sensitivity to DNA damage and replication stress of Tel1-deficient cells

(A) Exponentially growing cell cultures were serially diluted (1:10) and spotted out onto YEPD plates with or without camptothecin (CPT), hydroxyurea (HU), and methyl methanesulfonate (MMS) at the indicated concentrations.

(B) Appropriate dilutions of each cell culture were spread onto YEPD plates with or without CPT at the indicated concentrations. Plates were incubated 3 days at 25°C to determine the colony-forming units. Plotted values are the mean values with error bars denoting SD ($n = 3$).

(C) Appropriate dilutions of each cell culture were spread onto YEPD plates followed by the exposure to different UV doses. Plates were incubated 3 days at 25°C to determine the colony-forming units. Plotted values are the mean values with error bars denoting SD ($n = 3$).

(D) Cell cultures arrested in G2 with nocodazole were treated for 2 h with the indicated concentrations of phleomycin (noc+phleo), followed by spreading of phleomycin-treated and untreated cell cultures onto YEPD plates to determine the colony-forming units. Plotted values are the mean values with error bars denoting SD ($n = 3$).

(E) Appropriate dilutions of cell cultures with the indicated genotypes were spread onto YEPD plates containing the indicated concentrations of phleomycin (phleo), followed by determination of colony-forming units after 3 days at 25°C. Plotted values are the mean values with error bars denoting SD ($n = 3$).

(F) Exponentially growing cell cultures of the indicated strains were serially diluted (1:10) and spotted out onto YEPD plates with or without CPT, HU, and MMS.

EXO1 or *exo1-D171A* alleles did not affect the survival of both wild-type and *tel1Δ* cells to CPT, HU, and MMS in the presence of the endogenous *EXO1* gene (Figure S1E).[33] On the contrary, when the *exo1-D171A* allele was the only Exo1 source, it increased the sensitivity of *tel1Δ* cells to CPT, MMS, and HU similarly to *EXO1* deletion (Figure 1F), indicating that the Exo1 nuclease activity is essential to support cell viability of *tel1Δ* cells in response to genotoxic stress.

Here, we considered different possibilities that can explain the synthetic effect of Tel1 and Exo1 mutations in cell survival to genotoxic stress. First, Exo1 could support checkpoint activation in the absence of Tel1 kinase activity by promoting the activation of a Mec1-dependent checkpoint. Second, Exo1 could support DNA repair in the absence of Tel1. Third, the nuclease activity of Exo1 could become crucial for processing structures generated in the absence of Tel1 activity when replication forks are blocked by DNA lesions, torsional stress, or insufficient dNTPs levels.

Tel1 and Exo1 contribute to restrict a Mec1-dependent checkpoint

Since the kinase activity of Tel1 is essential only for some of the Tel1 functions,[23,25,27,45,52–56] but *tel1Δ exo1Δ* and *tel1-kd exo1Δ* cells show the same hypersensitivities to CPT, MMS, and HU (Figure 1A), we investigated how Exo1 supports the viability of *tel1-kd* cells. Furthermore, we focused on CPT treatment, because the lack of Exo1 and Tel1 activity strongly enhance the hypersensitivity to this agent.

Exo1 contributes to checkpoint activation in G1 or in the absence of functional Top1 and Top2 topoisomerases.[50,57,58] Since a Mec1-dependent checkpoint is activated in CPT-treated *tel1Δ* and *tel1-kd* cells,[33] Exo1 might support the viability of *tel1-kd* cells by contributing to the activation of this checkpoint. If this were the case, the lack of Exo1 should attenuate the Mec1-dependent checkpoint in CPT-treated *tel1-kd* cells. Alternatively, if Exo1 promotes DNA repair or the removal of intermediates generated at replication forks in the absence of Tel1, the absence of Exo1 should further enhance Mec1 activation in *tel1-kd* cells.

We have already shown that high CPT doses induced Rad53 phosphorylation in both *tel1Δ exo1Δ* cells and *tel1Δ* cells, suggesting that Exo1 does not contribute to activate the Mec1-dependent checkpoint in CPT.[33] However, checkpoint inactivation in these cells was not assessed. We now investigated checkpoint activation and switch off in wild-type and *tel1-kd* cells with or without *EXO1* by assessing the ability of cells to halt cell-cycle progression and phosphorylate the checkpoint effector kinase Rad53 after exposure to a sublethal dose of CPT. Checkpoint activation in CPT is known to delay nuclear division, without affecting the G1/S transition or the rate of bulk DNA replication.[33,59] When this checkpoint is switched off, we expect the cells to undergo nuclear division and cytokinesis and generate unbudded daughter cells. Cells were arrested in G1 with α-factor and released into fresh medium with or without CPT to analyze the kinetics of budding (Figures 2A and 2B), nuclear division (Figures 2C and 2D), and Rad53 phosphorylation (Figure 2E). Untreated cell cultures underwent budding (Figure 2A) and nuclear division with similar kinetics (Figure 2C). CPT treatment had no effect on bud formation in any cell culture (compare Figures 2A and 2B). A slight delay in nuclear division was observed in wild-type cells treated with CPT compared to untreated conditions (compare Figures 2C and 2D). The delay was extended in the absence of Exo1, and even more in the absence of Tel1 kinase activity (Figure 2D). Following nuclear division, wild-type, *exo1Δ*, and *tel1-kd* strains re-accumulated unbudded cells (Figure 2B), indicating the recovery from the checkpoint-mediated cell-cycle block. Strikingly, after 4 h from the release in CPT, approximately 90% of *tel1-kd exo1Δ* cells were still arrested as large-budded cells with undivided nuclei (Figures 2B and 2D), indicating that Exo1 inactivation exacerbated the cell-cycle delay caused by the *tel1-kd* allele. This persistent cell-cycle arrest correlated with a sustained Rad53 hyperphosphorylation in *tel1-kd exo1Δ* cells. In fact, slow-migrating Rad53 bands persisted longer in CPT-treated *tel1-kd exo1Δ* cells than in the other analyzed strains (Figures 2E and 2F).

The sustained checkpoint-dependent cell-cycle block caused by the inactivation of both Exo1 and of Tel1 kinase activity was confirmed by plating G1-arrested cells onto CPT-containing plates and monitoring the formation of microcolonies with more than two cells (Figure 2G). In fact, 80% of *tel1-kd exo1Δ* cells were arrested as large-budded cells for at least 4 h on CPT plates, while over 60% of *tel1-kd* cells and about 90% of wild-type and *exo1Δ* cells had recovered from the checkpoint arrest and formed microcolonies after 4 h on CPT-containing plates (Figure 2G). These findings indicate that the checkpoint is hyperactivated in CPT-treated *tel1-kd exo1Δ* cells compared to each single mutant. Therefore, Exo1 is not required for Mec1 activation in the absence of Tel1 activity but rather both Exo1 and Tel1 are required to resolve CPT-induced impediments.

The absence of Tel1 and Exo1 activities does not impair DSB repair by ectopic recombination

We asked if the increased DNA damage sensitivity and the checkpoint persistence of *tel1-kd exo1Δ* cells could be due to DNA repair defects. Exo1 participates in DNA MMR,[16,60,61] which is critical to repair mismatches that can arise during DNA replication and contributes to CPT resistance in mammals.[62,63] Therefore, the lack of Exo1 could exacerbate the phenotype of *tel1-kd* cells because it causes MMR defects. However, cells lacking Tel1 kinase activity and the core MMR factors, Mlh1 or Msh2, formed colonies as *tel1-kd* cells in the presence of CPT, HU, and MMS, and more efficiently that *tel1-kd exo1Δ* cells (Figure 3A), indicating that Exo1 supports the resistance of *tel1* mutant cells to genotoxic treatments independently of MMR.

Alternatively, the hypersensitivity and the checkpoint persistence in *tel1-kd exo1Δ* mutant cells could be due to DSB repair defects, considering that replication of parental DNA with trapped Top1 can generate DSBs and both Tel1 and Exo1 are involved in DSB repair by HR.[15,16,22,23] In particular, Tel1 and Exo1 were proposed to contribute to DSB end resection, as the lack of both Tel1 and Exo1 caused a severe resection defect when a site-specific DSB was induced in cells arrested in G2.[22] Although the lack of Tel1 itself delayed resection initiation, wild-type and *tel1-kd* cells process DNA ends with similar kinetics, suggesting that Tel1 kinase activity is dispensable for end resection.[23,27,64] However, we considered the possibility that a contribution of Tel1 kinase activity to resection might be overshadowed by the efficient processing exerted by Exo1 and, therefore, could be detected only in the absence of Exo1. To directly measure DSB end processing, we took advantage of the JKM139 background, where the *HO* gene is expressed from a galactose-inducible promoter and creates a single irreparable DSB at the *MATa* locus.[65] To get rid of potential effects caused by the cell-cycle phase on DSB processing, galactose was added to cells arrested and maintained in G2. ssDNA generation at the HO-induced DSB was assessed by Southern blotting under denaturing conditions as previously described (Figure S2A).[66] As expected,[23,27,64] DSB processing occurred with similar kinetics in both wild-type and *tel1-kd* cells (Figures 3B and 3C), whereas the 1.7 kb (r1) and 3.5 kb (r2) resection products accumulated in *exo1Δ* cells in which resection struggled to proceed beyond 3.5 kb from DSB ends (Figures 3B and 3C). These r1 and r2 resection bands accumulated with similar kinetics in *exo1Δ* and *tel1-kd exo1Δ* cells (Figures 3B and 3C), indicating that the lack of Exo1 and of Tel1 kinase activity do not have additive effects on resection kinetics in G2-arrested cells. Similar results were obtained when we monitored resection after HO induction and DSB formation in exponentially growing cells (Figures S2B and S2C). Therefore, while the lack of Tel1 synergizes with the lack of Exo1 for the resection defects,[22] the lack of Tel1 kinase activity does not. Despite the different DSB ends resection kinetics, *tel1Δ exo1Δ*, and *tel1-kd exo1Δ* cells exhibit the same
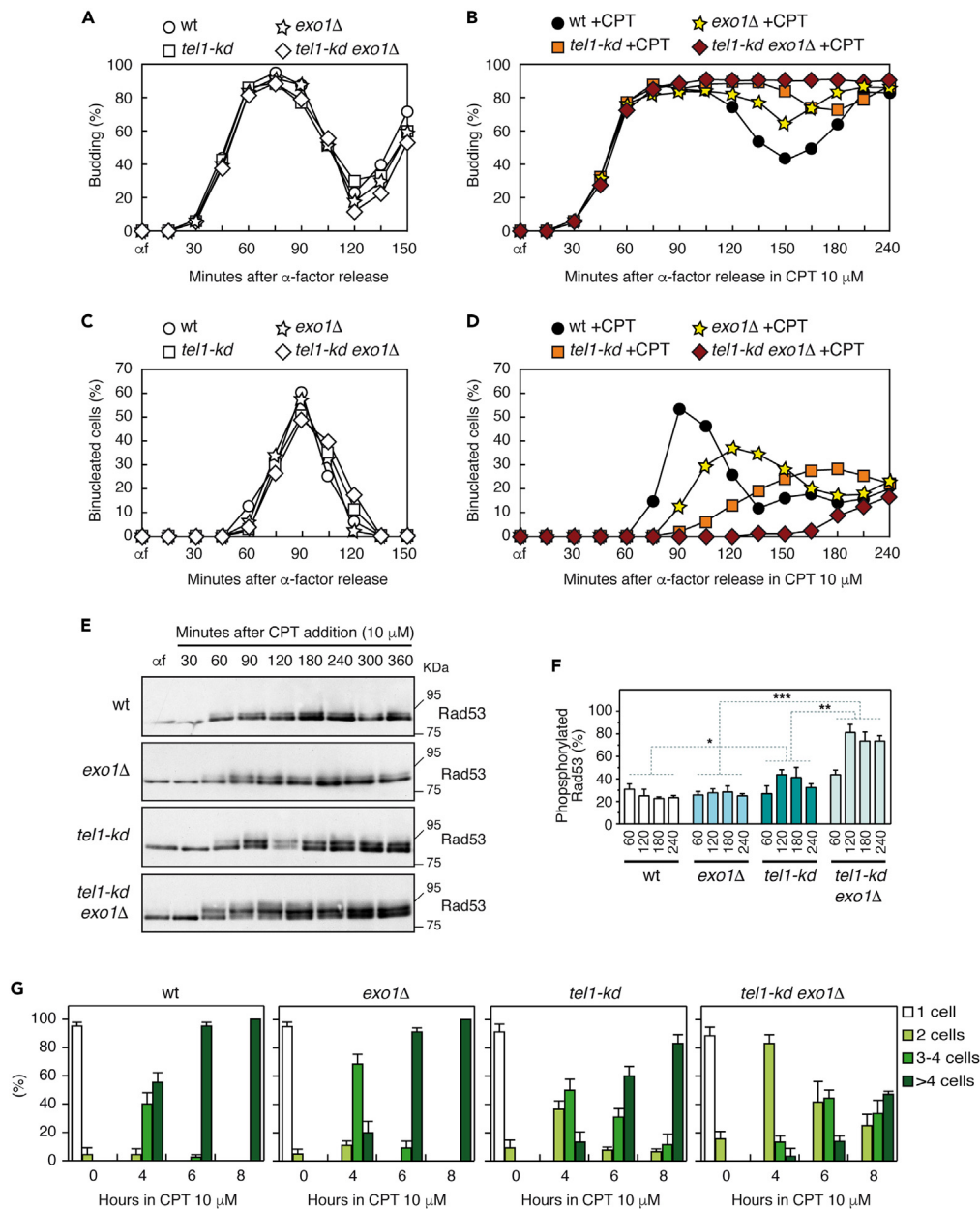
Figure 2. The lack of Exo1 and Tel1 extends the persistence of Mec1-dependent checkpoint activation in CPT

(A–F) Exponentially growing cell cultures were arrested in G1 with α-factor (αf) and released into YEPD with or without CPT (10 μM). Samples were harvested at the indicated time points to evaluate budding index by optical microscopy (A and B), or nuclear division by fluorescence microscopy (C and D), or Rad53 phosphorylation by western blot with anti-Rad53 antibodies (E). (F) Quantitative analysis of Rad53 phosphorylation was performed by calculating the ratio of band intensities for slowly–migrating bands to the total amount of protein. Plotted values are the mean values with error bars denoting SD ($n = 3$). Statistical analysis: Student's t test; $*p < 0.05$, $**p < 0.005$, and $***p < 0.001$.

(G) G1-arrested cell cultures were spread onto YEPD plates with CPT (10 μM). Microcolony formation was evaluated by optical microscopy at the indicated time points. The mean values are represented with error bars denoting SD ($n = 3$).

sensitivity to genotoxic treatments, suggesting that these sensitivities are likely not ascribable to the increased defect of *tel1Δ exo1Δ* cells in resecting DSB ends.

We also assessed whether the lack of Exo1 and Tel1 kinase activity affects HR by monitoring HO-induced ectopic recombination between two homologous DNA sequences located on different chromosomes in G2-arrested cells. We used a strain carrying the galactose-inducible *HO* gene, a *MAT* allele (*MATa-inc*) that cannot be cleaved by HO at chromosome III and an extra wild-type copy of the HO-cleavable *MATa*
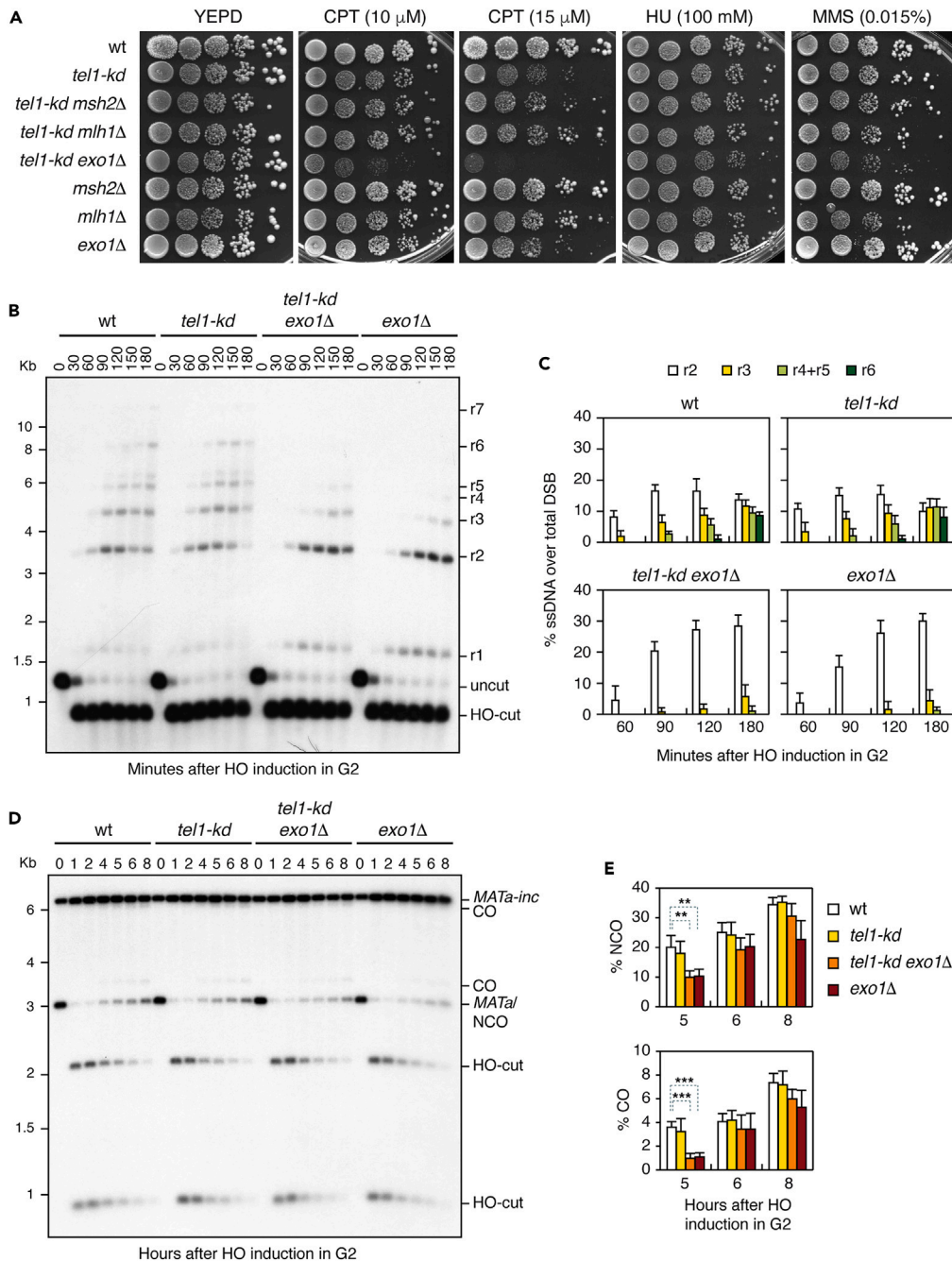
Figure 3. An HO-induced DSB is repaired in the absence of Exo1 and Tel1 activity

(A) Exponentially growing cell cultures of the indicated strains were serially diluted (1:10) and spotted out onto YEPD plates with or without CPT, HU, and MMS.

(B) YEPR JKM139 derivative strains were arrested in G2 with nocodazole and transferred to YEPRG at time zero in the presence of nocodazole. SspI-digested genomic DNA was hybridized with the *MATa* ss-RNA probe.

(C) Resection products in (B) were analyzed by densitometry. The mean values are represented with error bars denoting SD (*n* = 3).

(D) All the strains carry the deletion of the *LIG4* gene. G2-arrested YEPR cell cultures were transferred to YEPRG at time zero in the presence of nocodazole. Southern blot analysis of EcoRI-digested genomic DNA with a *MATa* probe.

(E) Densitometric analysis of NCO and CO band signals. Plotted values are the mean values with error bars denoting SD (*n* = 3). Statistical analysis: Student's t test; **p < 0.005 and ***p < 0.001.
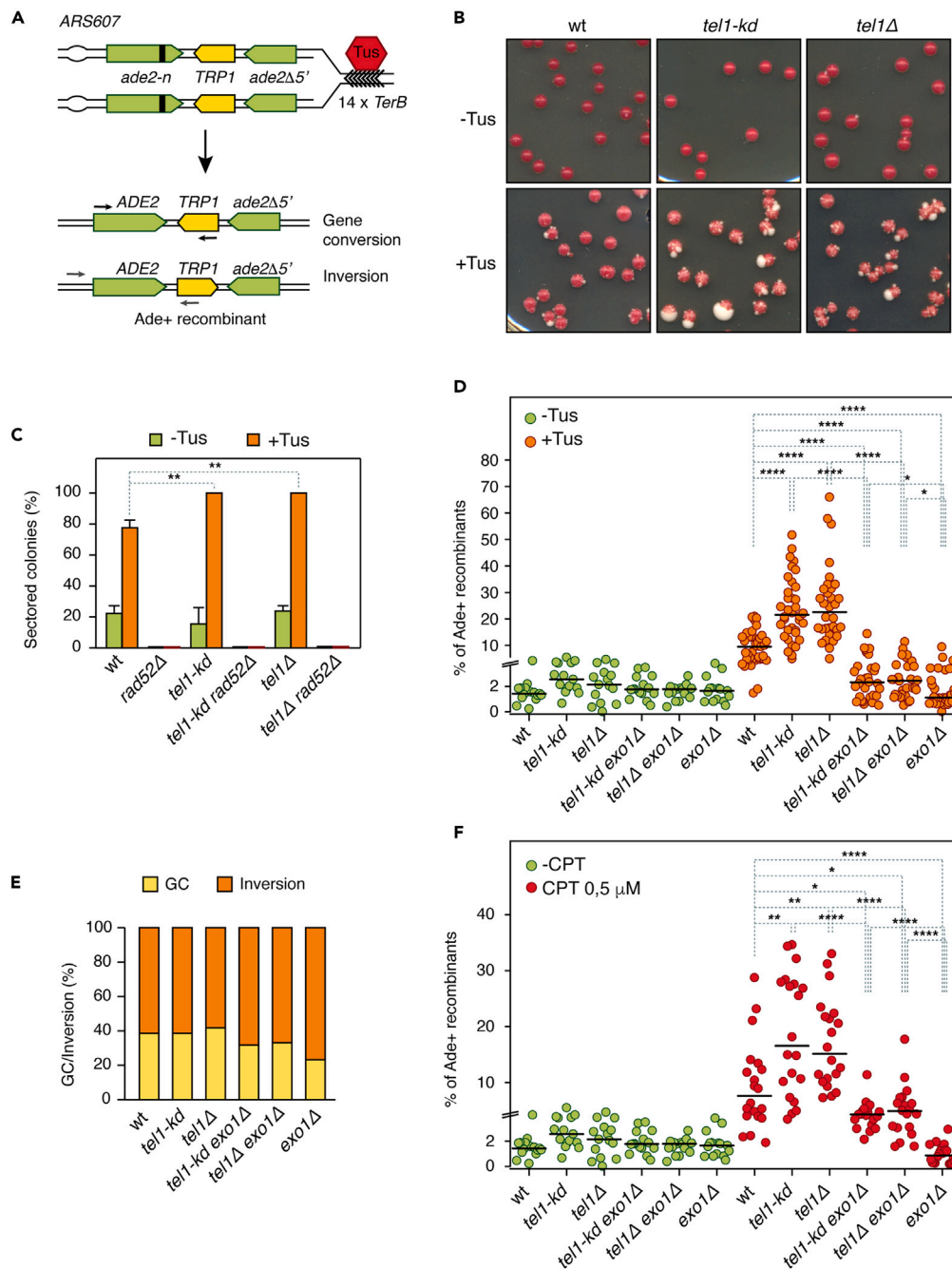
Figure 4. Tel1 limits recombination between inverted repeats at a stalled replication fork, whereas Exo1 promotes it

(A) Schematic representation of the *ade2* reporter and Tus/Ter barrier in the blocking orientation with regards to *ARS607*. The *ade2-n* allele carries a +2-frameshift mutation, indicated by a bold line. The *ade2-Δ5′* allele lacks the first 176 nucleotides and the promoter. Primers to score inversions and gene conversions are schematically represented.

(B) Strains with the indicated genotypes were plated on YEP plates containing glucose (−Tus) or galactose (+Tus). White sectors and papillae on red colonies are indicative of Ade+ phenotype.

(C) Quantitative analysis of red colonies with white sectors or papillae (indicative of Ade+ phenotype) to total colonies in the strains with the indicated genotypes. Plotted values are the mean values with error bars denoting SD (*n* = 3). Statistical analysis: Student's t test; **$p < 0.005$.

(D) Frequency of Ade+ recombinants without (green data points) and with (orange data points) induction of Tus expression with galactose. Black lines indicate medians. Statistical analysis: one-way ANOVA with a Bonferroni post-test; *$p < 0.05$ and ****$p < 0.0001$.

gene at chromosome V.[67] The HO-induced DSB on chromosome V can be repaired by HR using the homologous *MATa-inc* sequence on chromosome III as a donor, resulting in both noncrossover (NCO) and CO products (Figure S2D). In all the strains, the NHEJ ligase Lig4 was inactivated to abolish NHEJ contribution to the HO-induced DSB repair. CO and NCO products appeared with similar kinetics in wild-type and *tel1-kd* cells, indicating that Tel1 kinase activity is not required for ectopic recombination (Figures 3D and 3E). These products accumulated also in *exo1Δ* and *tel1-kd exo1Δ* cells with similar kinetics, although they appeared slightly later than in cells expressing wild-type *EXO1* (Figures 3D and 3E). This finding indicates that Tel1 kinase activity and Exo1 do not cooperate to repair a DSB by ectopic recombination in G2.

Tel1 counteracts Exo1-driven recombination between inverted repeats at a stalled replication fork

Besides inducing DSBs during DNA replication, CPT slows down the progression of replication forks and induces their reversal in both yeast and mammals.[29] Considering that reversed forks become unstable in the absence of Tel1, and this instability likely contributes to the sensitivity of *tel1* mutants to CPT,[33] Exo1 might support viability of *tel1* mutant cells to CPT by facilitating the recovery of DNA replication at unstable fork sites. To investigate this possibility, we employed the *Escherichia coli* Tus/Ter replication barrier that can induce a replication block in both yeast and mammals.[36,37,68–71] Similar to Top1 trapping on DNA induced by CPT, the Tus protein binding to *TerB* DNA repeats creates a transient barrier to the passage of the replication fork, thus stimulating mutagenesis, chromosomal rearrangements, and recombination events without necessarily causing DNA breaks.[68,69,71–74] Importantly, both CPT and Tus/Ter barrier were proposed to induce fork reversal.[29,37,71]

To explore whether Tel1 and Exo1 regulate Tus/Ter-induced recombination between inverted DNA repeats, we took advantage of strains in which the *TUS* gene is expressed from a galactose-inducible promoter and 14 *TerB* repeats are located on chromosome VI in the blocking orientation respect to *ARS607*, and adjacent to a reporter system with two *ade2* heteroalleles separated by a *TRP1* gene (Figure 4A).[71] Cells with this genetic background display an Ade− phenotype and form red colonies (Figure 4B),[75] whereas recombination between the inverted *ade2* alleles can result in the formation of a wild-type *ADE2* gene and of Ade+ white offspring (Figures 4A and 4B). Since the lack of the core recombination factor Rad52 results in the formation of red colonies only (Figure 4C),[71] the presence of Ade+ white colonies or white sectors within a red colony serves as a readout for non-allelic HR events.

Exponentially growing cell cultures were spread either on glucose-containing plates, where the *TUS* gene is repressed (−Tus), and on galactose-containing plates (+Tus), where the expression of the *TUS* gene is induced, and plates were incubated 3–4 days at 30°C. The appearance of white or sectored colonies on glucose- and galactose-containing plates was indicative of spontaneous or replication block-induced recombination between the inverted *ade2* repeats, respectively. Single colonies of similar size from the different plates were diluted and a fixed number of cells were spread on YEPD plates and on selective medium lacking adenine to evaluate the frequency of Ade+ recombinants both in the presence and absence of Tus induction. Consistent with previous findings,[71] an increased proportion of colonies with white sectors formed on galactose-containing plates (+Tus), compared to YEPD plates (−Tus) (Figures 4B and 4C), and Tus expression increased the recombination frequency from 1.43% to 9.47% in wild-type cells (Figure 4D; Table S1). As the contribution of Tel1 in the regulation of recombination between inverted repeats near a stalled fork was not assessed before, we evaluated recombination frequencies in both *tel1Δ* and *tel1-kd* cells. Notably, both the proportion of sectored colonies on galactose-containing plates (Figures 4B and 4C) and the frequency of Ade+ colonies after galactose addition increased in the absence of Tel1 or its kinase activity (22.57% for *tel1Δ* cells and 21.55% for *tel1-kd* cells) (Figure 4D, +Tus; Table S1). Rad52 was absolutely required for the formation of sectored colonies in the absence of Tel1 or its kinase activity (Figure 4C), indicating that they result from recombination events. Importantly, the lack of Tel1 or its kinase activity did not increase the percentage of both sectored colonies (Figures 4B and 4C) and Ade+ colonies when Tus was not expressed (Figure 4D, −Tus; Table S1), indicating that Tel1 does not limit spontaneous recombination. Therefore, the anti-recombination activity of Tel1 is specifically triggered by the replication block. We can conclude that Tel1 kinase activity constrains recombination events between inverted repeats near stalled replication forks.

Interestingly, spontaneous recombination between inverted repeats was found to require Mre11 and not Exo1, while Exo1 is strictly required for recombination events stimulated by a replication block, which are only partially reduced in the absence of Mre11.[71] As we found that Tel1 restricts recombination specifically after the induction of a replication fork barrier, we asked whether Exo1 is required for these recombination events. Indeed, it is, as the absence of Exo1 reduced the frequency of Ade+ recombinants in both galactose-induced wild-type and *tel1* mutant cells to levels comparable to those observed in non-induced cells (Figure 4D). In conclusion, replication fork stalling at a polar Tus/Ter barrier stimulates Exo1-mediated recombination between inverted repeats, while Tel1 counteracts these recombination processes through its kinase activity.

Ade+ recombinants can arise through either gene conversion or inversion of the *TRP1* locus, and Tus expression in wild-type cells was found to induce both events almost equally.[71] We sought to determine whether Tel1 specifically counteracts one of these processes and whether they both require Exo1. The nature of Tus/Ter-induced recombination events was assessed in approximately 30 independent Ade+ recombinants from each genomic background through PCR reactions performed by using pairs of primers specific for gene conversion

or inversion products (Figure 4A).[71] The absence of Tel1 or its kinase activity did not alter the proportion of the two events compared to the wild-type strain. In fact, the PCR products corresponding to inversions were observed in approximately 60% of wild-type, tel1-kd, and tel1Δ Ade+ recombinants, while the remaining 40% exhibited gene conversions (Figure 4E; Table S2). Both gene conversions and inversions were also detectable in the rare tel1-kd exo1Δ, tel1Δ exo1Δ, and exo1Δ Ade+ recombinants, although the proportion of gene conversions in favor of inversions was slightly reduced compared to strains expressing wild-type Exo1 (Figure 4E; Table S2). We can conclude that the increased recombination frequency in tel1-mutant cells is not attributable to the hyperactivation of specific recombination processes.

Tel1 restricts Exo1-mediated recombination between inverted repeats near *ARS607* in CPT

Interestingly, the same HR events triggered by the Tus/Ter barrier near *ARS607* can be stimulated by genome-wide replication stress, such as the one imposed by MMS or CPT treatment.[71] We asked whether the lack of Tel1 or of its kinase activity also increases the frequency of recombination between inverted repeats near *ARS607* in CPT. When wild-type, tel1Δ, and tel1-kd cells were spread onto YEPD plates with or without CPT, an increased proportion of colonies containing white sectors became clearly visible on CPT-containing plates compared to YEPD plates (Figure S3). Quantification of Ade+ recombinants revealed that in wild-type cells recombination frequency increased from 1.43%, under untreated conditions, to 7.59% in the presence of CPT (Figure 4F; Table S1). Similar to what was observed after the induction of the Tus/Ter barrier, recombination events between inverted repeats that are stimulated by topoisomerase poisoning require Exo1, whose lack strongly reduced recombination frequency to the levels observed in untreated cells (Figure 4F; Table S1). Conversely, the frequency of Ade+ recombinants significantly increased from 2.15% to 15.11% and from 2.57% to 16.54% in cells lacking Tel1 or its kinase activity, respectively (Figure 4F; Table S1). HR events in tel1 mutants are strongly dependent on Exo1, whose absence reduced the frequency of Ade+ recombinants in tel1Δ and tel1-kd cells to 4.88% and 4.28%, respectively (Figure 4F; Table S1). These findings indicate that Tel1 prevents or restricts HR between inverted repeats in the presence of genome-wide torsional stress, and that Exo1 promotes hyper-recombination in the absence of Tel1 activity.

The Mre11 nuclease activity and Ku contribute to hyper-recombination at a stalled replication fork in Tel1-deficient cells

Since the nuclease activity of Mre11 was found to be responsible for the instability of reversed forks in the absence of Tel1,[33] we tested the effect of the absence of Mre11 nuclease activity in tel1 mutants. We considered that if reversed fork instability stimulates recombination between inverted repeats at the Tus/Ter barrier, the absence of Mre11 nuclease activity would reduce the elevated recombination rate observed in tel1 mutants to wild-type levels. Indeed, the frequency of Tus/Ter-induced Ade+ recombinants in tel1Δ and tel1-kd cells expressing the nuclease-dead Mre11-H125N variant[76] was significantly lower compared to tel1Δ and tel1-kd cells (7.5% and 11.32% compared to 22.57% and 21.55%, respectively) and similar to that observed in wild-type and mre11-H125N cells (9.47% and 7.37, respectively) (Figure 5A; Table S1). The finding that the lack of Mre11 nuclease activity did not significantly reduce the replication block-induced recombination compared to wild-type cells indicates that Mre11 nuclease activity promotes HR between inverted repeats specifically in Tel1-deficient cells.

In both yeast and mammals, the processing of stalled or broken replication forks is negatively regulated by the Ku heterodimer, which is known to counteract Exo1-mediated DNA end resection.[77–85] As Tel1 kinase activity stimulates the removal of the Ku heterodimer from the DNA ends,[25,28] we investigated the contribution of Ku in the Tus/Ter-induced recombination both in the presence and in the absence of Tel1 kinase activity. As the inactivation of Ku and of Tel1 or its kinase activity causes a reduced viability also at the permissive temperature of 25°C, due to telomere shortening and precocious replicative senescence (Figure S4A),[86] we used the ku70-Y494N allele, which reduces the binding of Ku with DNA ends and allows Exo1 to resect DSB ends.[25,87] This allele was inserted in the strain carrying the Tus/Ter inducible system and the inverted ade2 repeats, alone or in combination with tel1-kd allele. Experiments to evaluate spontaneous and Tus/Ter-induced recombination were carried out as described previously but at 25°C. At this temperature, the ability of tel1-kd ku70-Y494N cells to form colonies was only slightly reduced compared to wild-type and tel1-kd and ku70-Y494N single mutant cells (Figures S4B and S4C).

The Ku-Y494N variant, which per se did not affect the rate of both spontaneous and replication block-induced recombination, reduced the formation of Ade+ recombinants in galactose-induced tel1-kd cells (Figure 5B; Table S3), indicating that Ku contributes to the hyper-recombination at stalled forks in the absence of Tel1 kinase activity. Although the ku70-Y494N mutation reduced to wild-type levels the hyper-recombination caused by the tel1-kd allele, this mutation did not restore the resistance of tel1-kd cells to genotoxic agents, but rather tel1-kd ku70-Y494N cells were more sensitive to CPT, HU, and MMS than both tel1-kd and ku70-Y494N cells (Figure S4C). As the DNA binding of Ku70 is required both for NHEJ and DSB end tethering, and both Ku and Tel1 promote DNA end tethering that supports DSB repair,[25,87] the hypersensitivity of tel1-kd ku70-Y494N cells could be due to a defect in DSB repair. Alternatively, it could simply result from the slow growth phenotype of these cells, whose growth was slightly defective at 25°C and strongly reduced at higher temperatures (Figure S4B).

As both ku70-Y494N and mre11-H125N mutations reduced the hyper-recombination in tel1-kd cells to similar extents, we asked whether they act in the same or in different pathways for Tus/Ter-induced recombination. We therefore generated strains carrying both the ku70-Y494N and mre11-H125N alleles and the tel1-kd mutations. Interestingly, tel1-kd ku70-Y494N mre11-H125N cells generates Ade+ recombinants as tel1-kd ku70-Y494N and tel1-kd mre11-H125N cells (8.13%, 7.32%, and 12.3%, respectively) and significantly less than tel1-kd cells (24.56%) (Figure 5B; Table S3). Therefore, the nuclease activity of Mre11 and the DNA end binding capacity of Ku appear to sustain hyper-recombination at stalled forks in the absence of Tel1 kinase activity by acting in the same pathway.

Altogether, our findings indicate that Tel1 exerts an anti-recombination activity at stalled replication forks, likely by stabilizing intermediates that aid in the resumption of DNA replication. In the absence of Tel1, these intermediates are exposed to Mre11 and Exo1 activities, as well as to Ku-dependent control, that channel them into HR events.
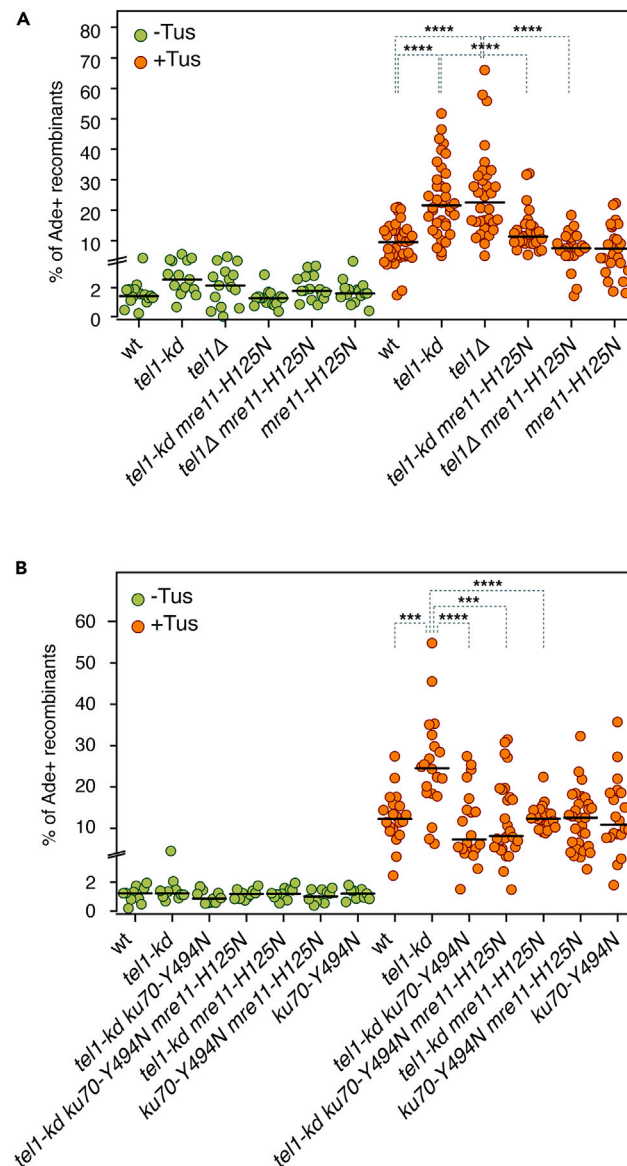
Figure 5. The Mre11 nuclease activity and Ku promote recombination between inverted repeats near early replication origins

(A and B) Frequency of Ade+ recombinants without (green data points) and with (orange data points) induction of Tus expression. Black lines indicate medians. Statistical analysis: one-way ANOVA with a Bonferroni post-test; ***$p < 0.001$ and ****$p < 0.0001$.

DISCUSSION

In this study, we found that Exo1 nuclease activity supports the viability of Tel1-deficient cells to compounds that hinder DNA replication, and particularly to CPT and MMS, which can induce replication fork stalling and reversal, and replication-born DSBs.[29,73,88–90] Furthermore, Exo1 supports Tel1 in restricting the activation of a Mec1-dependent checkpoint in CPT, suggesting an interplay between Tel1 and Exo1 in removing toxic ssDNA-rich structures caused by Top1 trapping onto DNA. *tel1 exo1* mutant cells do not exhibit increased defects in either processing or repair of an endonuclease-induced DSB compared to *tel1* and *exo1* single mutant cells. This suggests that the strong hyper-sensitivities caused by both Tel1 and Exo1 inactivation are not due to increased DSB repair defects. Rather, we found that Tel1, through its kinase activity, restricts HR events between inverted repeats when a replication fork stalls because of CPT treatment or the induction of Tus/Ter barrier, which both cause a transient stabilization of protein-DNA complexes, fork reversal, and recombination between inverted repeats.[29,36,37,68–71,73] Exo1 and Mre11 nucleases, as well as the Ku complex, are responsible for this hyper-recombination in Tel1-deficient cells, suggesting that Tel1 limits the generation of intermediates that trigger Mre11- and Exo1-dependent recombination events associated with chromosome rearrangements. These events likely support the completion of DNA replication and cell survival, albeit at the cost of increased genome instability.
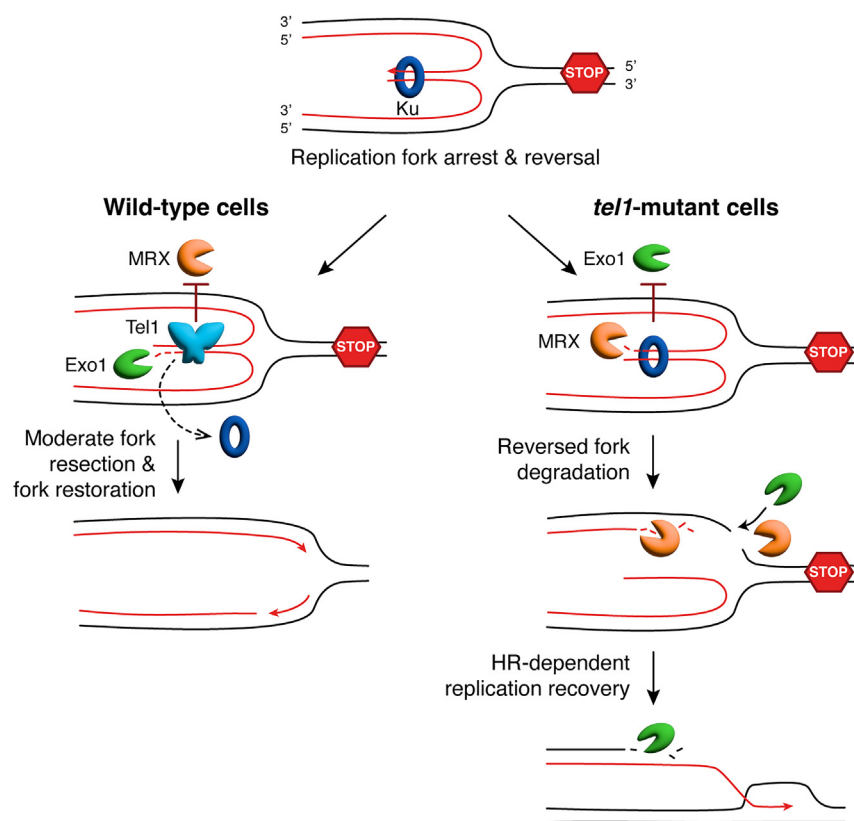
Figure 6. Model for the interplays between Tel1, Exo1, Ku and MRX at stalled replication forks

Fork reversal ahead a replication block leads to the recruitment of Ku and Tel1, which restrict the action of Exo1 and MRX, respectively. By promoting Ku release from the regressed arm, Tel1 allows a controlled degradation of nascent strands by Exo1, which, in turn, promotes the restoration of a functional fork through either fork remodeling or HR within the parental duplex (left). The absence of Tel1 maintains Exo1 inhibition induced by Ku persistence at the regressed arm, while an unrestricted Mre11 nucleolytic activity can either extensively degrade nascent DNA strands or cleave the branched structure. Exo1 can access to the intermediates generated by the unscheduled MRX action at reversed forks, and, through its 5'-3' exonucleolytic activity, can generate 3'-ended ssDNA tails that trigger HR in the presence of homologous sequences.

We have previously observed a decrease in the number of reversed forks in CPT-treated Tel1-deficient cells compared to wild-type cells.[33] Furthermore, the inactivation of Mre11 nuclease restores the levels of reversed forks in Tel1-deficient cells to those observed in wild-type cells, suggesting that Tel1 has a protective function against reversed forks degradation by Mre11. In contrast, Exo1 was found to be dispensable for reversed forks disruption in Tel1-deficient cells, as the absence of Exo1 does not increase the levels of the reversed forks in *tel1* mutant cells.[33] Our finding that both Mre11 and Exo1 are required for HR events induced by fork stalling in Tel1-deficient cells, while Mre11, but not Exo1, participates in reversed fork degradation, suggests that Exo1 does not directly act on the regressed arms of the reversed forks, but possibly it promotes HR by processing other structures generated at stalled forks. These structures are likely more abundant in the absence of Tel1 activity. In fact, Exo1 is required for fork stalling-induced recombination between inverted repeats both in wild-type cells and in cells with dysfunctional Tel1. On the contrary, the lack of Mre11 nuclease activity reduced Tus/Ter-induced recombination in *tel1* mutants to wild-type levels without affecting recombination in wild-type cells, suggesting that Mre11 activity generates the structures that require Exo1 processing to be channeled into HR. The inability of Exo1 to degrade reversed forks in the absence of Tel1 might be attributed to the persistence of the Ku heterodimer at these structures. In fact, Ku is known to counteract resection of stalled or broken replication forks in both yeast and mammals,[77–85] and its binding/persistence at DNA ends has been shown to be restricted by the Tel1 kinase activity.[25] We found that a reduction of Ku70 DNA end-binding activity relieves the hyper-recombination at stalled forks in *tel1-kd* cells without affecting recombination in the presence of wild-type Tel1, and that Ku and Mre11 appear to act in the same pathway in limiting hyper-recombination in the absence of Tel1 activity. These findings suggest that the persistence of Ku complex at regressed DNA ends in the absence of Tel1 somehow allows Mre11-dependent degradation of the stalled fork. This unscheduled Mre11 action can be due to a positive regulation exerted by Ku on Mre11 or by the fact that Ku persistence inhibits the action of Exo1 on the regressed arm, thus favoring an Mre11-dependent processing of the reversed fork.

Altogether, these data support a model in which reversed forks, which form ahead a replication block, engage Ku, which limits Exo1 action on the regressed arm, while Tel1 counteracts the Mre11 nucleolytic function through its kinase activity (Figure 6). Similar to what was observed

at DSBs,[25] Tel1 can promote Ku removal from the regressed arm, thus allowing the access of Exo1.[31,32] Therefore, the presence of Tel1 and Ku at reversed forks and the interplays between these two factors can result in a controlled degradation of nascent strands by Exo1 and possibly Mre11, which is necessary to restore a functional fork through either fork remodeling or HR within the parental duplex. In the absence of Tel1, Ku persistence at the regressed arm could prevent the action of Exo1 but not of Mre11. The unrestricted Mre11 nucleolytic activity might disrupt the reversed structure, either by excessively degrading nascent DNA strands or cleaving the branched structure. Given that both Mre11 and Exo1 are required for HR between inverted repeats in the absence of Tel1, we propose that structures generated in *tel1* mutants by an unscheduled MRX action at reversed forks can represent suitable substrates for Exo1. Through its 5′-3′ exonucleolytic activity, Exo1 generates 3′-ended ssDNA tails capable of searching for homologous sequences, thereby facilitating their engagement in HR events (Figure 6). Structures generated in the absence of both Tel1 and Exo1 are not channeled into HR, possibly because the ssDNA tails are either too short to stably pair with homologous sequences or terminate with 5′-overhangs that are unsuitable for initiating DNA synthesis. The persistence of these aberrant structures can lead to cell death either by impeding the recovery of DNA replication or by inducing toxic genetic instability.

How Mre11 disrupts reversed forks in the absence of Tel1 is still unclear. It can either degrade the nascent leading strand through its 3′ to 5′ exonucleolytic activity or cleave the branched structure with its endonucleolytic activity (Figure 6). This cleavage could be achieved in conjunction with structure-specific nucleases, such as Mus81-Mms4 and Yen1.[91,92] Cleaved molecules are potential substrates for Exo1, which removes mononucleotides from the 5′-end of blunt-ended, 5′-recessed termini, DNA nicks, and DNA structures carrying a flap with a 5′ overhang.[93] Homology-dependent mechanisms triggered by Exo1 can either restore a functional replication fork or repair the broken DNA strand, whose replication is then accomplished by an incoming replication fork in the opposite direction.

Interestingly, Tel1 was proposed to counteract genetic instability triggered by replication errors or replication fork stalling at telomeres. Indeed, Tel1 deficiency was found to enhance recombination and chromosome instability, and this instability was further increased in the absence of the helicase Rrm3, that prevents fork stalling.[94] It will be intriguing to evaluate whether Exo1 can be responsible for instability triggered at telomeres in the absence of Tel1.

It is known that ATM and EXO1 play crucial and evolutionarily conserved functions in genome integrity mechanisms also in mammals, where germline mutations in these genes are associated with increased cancer susceptibilities.[95–98] From yeast to mammals, EXO1 plays a major function in generating 3′-ended ssDNA overhangs during several DNA damage repair pathways, including MMR, nucleotide excision repair, base excision repair, and both mitotic and meiotic recombination.[16,38,39,93] As yeast Tel1, ATM activates HR pathway for repair of DNA DSBs and participates to the metabolism of reversed forks, which are common intermediates of both unperturbed and stressed DNA replication, and requires EXO1-mediated processing.[29,31,43,90,97] Notably, EXO1 was recently found to support the viability of BRCA1-deficient cells and cells lacking both BRCA1 and EXO1 activities accumulate replication-associated DNA lesions.[99] It will be interesting to assess whether EXO1 supports ATM functions in response to replication stress, as our findings in yeast suggest. As ATM dysfunctions sensitize cancer cells to radiations and ATM inhibition is considered as a promising strategy for cancer therapy,[97] a synthetic genetic interaction between *EXO1* and *ATM* mutations suggests that therapy of tumors with *EXO1* mutations can benefit of ATM inhibition.

Limitations of the study

The finding that Tel1 kinase activity is required for the anti-recombination function at stalled forks indicates that Tel1 limits HR through the phosphorylation of specific substrates. The identity of these factors remains to be defined. An intriguing possibility is that they include chromatin remodeling factors, as Tel1 was proposed to regulate nucleosome eviction at DNA DSBs,[25] and chromatin modifiers were recently involved in reversed forks protection.[37]

In addition, how Exo1 triggers the resolution of intermediates generated in *tel1* mutants remains to be elucidated. Besides promoting extensive resection of DSB ends, Exo1 promotes nucleotide excision repair and error free post replicative repair.[39,51,58,100,101] The activation of one or a combination of these pathways can promote the survival of Tel1-deficient cells to CPT.

STAR★METHODS

Detailed methods are provided in the online version of this paper and include the following:

- KEY RESOURCES TABLE
- RESOURCE AVAILABILITY
  - Lead contact
  - Materials availability
  - Data and code availability
- EXPERIMENTAL MODEL AND STUDY PARTICIPANT DETAILS
- METHOD DETAILS
  - Spot assays and colony formation assay
  - Analysis of cell-cycle progression and western blotting
  - Microcolony formation assay
  - Double-strand break end resection
  - Double-strand break repair by ectopic recombination

- ○ Measurement of Ade+ recombination frequencies
- ○ Distribution of Ade+ recombinants
- ● QUANTIFICATION AND STATISTICAL ANALYSIS
- ○ Statistical analysis

AUTHOR CONTRIBUTIONS

Conceptualization, M.G., M.P.L., and M.C.; investigation, M.G., C.F., C.V.C., and E.C.; writing – original draft, M.C.; writing – review & editing, M.G., M.P.L., and M.C.; supervision, M.C.; funding acquisition, M.P.L. and M.C.

DECLARATION OF INTERESTS

The authors declare no competing interests.

REFERENCES

1. Matsuoka, S., Ballif, B.A., Smogorzewska, A., McDonald, E.R. 3rd, Hurov, K.E., Luo, J., Bakalarski, C.E., Zhao, Z., Solimini, N., Lerenthal, Y., et al. (2007). ATM and ATR substrate analysis reveals extensive protein networks responsive to DNA damage. Science *316*, 1160–1166. https://doi.org/10.1126/science.1140321.

2. Smolka, M.B., Albuquerque, C.P., Chen, S.H., and Zhou, H. (2007). Proteome-wide identification of in vivo targets of DNA damage checkpoint kinases. Proc. Natl. Acad. Sci. USA *104*, 10364–10369. https://doi.org/10.1073/pnas.0701622104.

3. Scully, R., Panday, A., Elango, R., and Willis, N.A. (2019). DNA double-strand break repair-pathway choice in somatic mammalian cells. Nat. Rev. Mol. Cell Biol. *20*, 698–714. https://doi.org/10.1038/s41580-019-0152-0.

4. Williams, R.M., and Zhang, X. (2021). Roles of ATM and ATR in DNA Double Strand Breaks and Replication Stress. Prog. Biophys. Mol. Biol. *163*, 109–119. https://doi.org/10.1016/j.pbiomolbio.2021.03.007.

5. Colombo, C.V., Gnugnoli, M., Gobbini, E., and Longhese, M.P. (2020). How do cells sense DNA lesions? Biochem. Soc. Trans. *48*, 677–691. https://doi.org/10.1042/BST20191118.

6. Pizzul, P., Casari, E., Gnugnoli, M., Rinaldi, C., Corallo, F., and Longhese, M.P. (2022). The DNA damage checkpoint: A tale from budding yeast. Front. Genet. *13*, 995163. https://doi.org/10.3389/fgene.2022.995163.

7. Zou, L., and Elledge, S.J. (2003). Sensing DNA damage through ATRIP recognition of RPA-ssDNA complexes. Science *300*, 1542–1548. https://doi.org/10.1126/science.1083430.

8. Deshpande, I., Seeber, A., Shimada, K., Keusch, J.J., Gut, H., and Gasser, S.M. (2017). Structural Basis of Mec1-Ddc2-RPA Assembly and Activation on Single-Stranded DNA at Sites of Damage. Mol. Cell. *68*, 431–445.e5. https://doi.org/10.1016/j.molcel.2017.09.019.

9. Shiotani, B., and Zou, L. (2009). Single-stranded DNA orchestrates an ATM-to-ATR switch at DNA breaks. Mol. Cell. *33*, 547–558. https://doi.org/10.1016/j.molcel.2009.01.024.

10. Fukunaga, K., Kwon, Y., Sung, P., and Sugimoto, K. (2011). Activation of protein kinase Tel1 through recognition of protein-bound DNA ends. Mol. Cell Biol. *31*, 1959–1971. https://doi.org/10.1128/MCB.05157-11.

11. Hailemariam, S., Kumar, S., and Burgers, P.M. (2019). Activation of Tel1ATM kinase requires Rad50 ATPase and long nucleosome-free DNA but no DNA ends. J. Biol. Chem. *294*, 10120–10130. https://doi.org/10.1074/jbc.RA119.008410.

12. Mehta, A., and Haber, J.E. (2014). Sources of DNA double-strand breaks and models of recombinational DNA repair. Cold Spring Harbor Perspect. Biol. *6*, a016428. https://doi.org/10.1101/cshperspect.a016428.

13. Emerson, C.H., and Bertuch, A.A. (2016). Consider the workhorse: Nonhomologous end-joining in budding yeast. Biochem. Cell. Biol. *94*, 396–406. https://doi.org/10.1139/bcb-2016-0001.

14. Cannavo, E., and Cejka, P. (2014). Sae2 promotes dsDNA endonuclease activity within Mre11–Rad50–Xrs2 to resect DNA breaks. Nature *514*, 122–125. https://doi.org/10.1038/nature13771.

15. Mimitou, E.P., and Symington, L.S. (2008). Sae2, Exo1 and Sgs1 collaborate in DNA double-strand break processing. Nature *455*, 770–774. https://doi.org/10.1038/nature07312.

16. Zhu, Z., Chung, W.H., Shim, E.Y., Lee, S.E., and Ira, G. (2008). Sgs1 Helicase and Two Nucleases Dna2 and Exo1 Resect DNA Double-Strand Break Ends. Cell *134*, 981–994. https://doi.org/10.1016/j.cell.2008.08.037.

17. Cejka, P., Cannavo, E., Polaczek, P., Masuda-Sasa, T., Pokharel, S., Campbell, J.L., and Kowalczykowski, S.C. (2010). DNA end resection by Dna2–Sgs1–RPA and its stimulation by Top3–Rmi1 and Mre11–Rad50–Xrs2. Nature *467*, 112–116. https://doi.org/10.1038/nature09355.

18. Niu, H., Chung, W.H., Zhu, Z., Kwon, Y., Zhao, W., Chi, P., Prakash, R., Seong, C., Liu, D., Lu, L., et al. (2010). Mechanism of the ATP-dependent DNA end-resection machinery from Saccharomyces cerevisiae. Nature *467*, 108–111. https://doi.org/10.1038/nature09318.

19. Garcia, V., Phelps, S.E., Gray, S., and Neale, M.J. (2011). Bidirectional resection of DNA double-strand breaks by Mre11 and Exo1. Nature *479*, 241–244. https://doi.org/10.1038/nature10515.

20. Ritchie, K.B., Mallory, J.C., and Petes, T.D. (1999). Interactions of TLC1 (which encodes the RNA subunit of telomerase), TEL1, and MEC1 in regulating telomere length in the yeast Saccharomyces cerevisiae. Mol. Cell Biol. *19*, 6065–6075.

21. Galli, M., Frigerio, C., Longhese, M.P., and Clerici, M. (2021). The regulation of the DNA

damage response at telomeres: focus on kinases. Biochem. Soc. Trans. *49*, 933–943. https://doi.org/10.1042/BST20200856.

22. Mantiero, D., Clerici, M., Lucchini, G., and Longhese, M.P. (2007). Dual role for Saccharomyces cerevisiae Tel1 in the checkpoint response to double-strand breaks. EMBO Rep. *8*, 380–387. https://doi.org/10.1038/sj.embor.7400925.

23. Cassani, C., Gobbini, E., Wang, W., Niu, H., Clerici, M., Sung, P., and Longhese, M.P. (2016). Tel1 and Rif2 regulate MRX functions in end-tethering and repair of DNA double-strand breaks. PLoS Biol. *14*, e1002387. https://doi.org/10.1371/journal.pbio.1002387.

24. Mimitou, E.P., Yamada, S., and Keeney, S. (2017). A global view of meiotic double-strand break end resection. Science *355*, 40–45. https://doi.org/10.1126/science.aak9704.

25. Rinaldi, C., Pizzul, P., Casari, E., Mangiagalli, M., Tisi, R., and Longhese, M.P. (2023). The Ku complex promotes DNA end-bridging and this function is antagonized by Tel1/ATM kinase. Nucleic Acids Res. *51*, 1783–1802. https://doi.org/10.1093/nar/glab065.

26. Pizzul, P., Casari, E., Rinaldi, C., Gnugnoli, M., Mangiagalli, M., Tisi, R., and Longhese, M.P. (2024). Rif2 interaction with Rad50 counteracts Tel1 functions in checkpoint signalling and DNA tethering by releasing Tel1 from MRX binding. Nucleic Acids Res. *52*, 2355–2371. https://doi.org/10.1093/nar/gkad1246.

27. Gobbini, E., Villa, M., Gnugnoli, M., Menin, L., Clerici, M., and Longhese, M.P. (2015). Sae2 Function at DNA Double-Strand Breaks Is Bypassed by Dampening Tel1 or Rad53 Activity. PLoS Genet. *11*, e1005685. https://doi.org/10.1371/journal.pgen.1005685.

28. Iwasaki, D., Hayashihara, K., Shima, H., Higashide, M., Terasawa, M., Gasser, S.M., and Shinohara, M. (2016). The MRX Complex Ensures NHEJ Fidelity through Multiple Pathways Including Xrs2-FHA-Dependent Tel1 Activation. PLoS Genet. *12*, e1005942. https://doi.org/10.1371/journal.pgen.1005942.

29. Ray Chaudhuri, A., Hashimoto, Y., Herrador, R., Neelsen, K.J., Fachinetti, D., Bermejo, R., Cocito, A., Costanzo, V., and Lopes, M. (2012). Topoisomerase I poisoning results in PARP-mediated replication fork reversal. Nat. Struct. Mol. Biol. *19*, 417–423. https://doi.org/10.1038/nsmb.2258.

30. Neelsen, K.J., and Lopes, M. (2015). Replication fork reversal in eukaryotes: from dead end to dynamic response. Nat. Rev. Mol. Cell Biol. *16*, 207–220. https://doi.org/10.1038/nrm3935.

31. Berti, M., Cortez, D., and Lopes, M. (2020). The plasticity of DNA replication forks in response to clinically relevant genotoxic stress. Nat. Rev. Mol. Cell Biol. *21*, 633–651. https://doi.org/10.1038/s41580-020-0231-9.

32. Ait Saada, A., Lambert, S.A.E., and Carr, A.M. (2018). Preserving replication fork integrity and competence via the homologous recombination pathway. DNA Repair *71*, 135–147. https://doi.org/10.1016/j.dnarep.2018.08.017.

33. Menin, L., Ursich, S., Trovesi, C., Zellweger, R., Lopes, M., Longhese, M.P., and Clerici, M. (2018). Tel1/ATM prevents degradation of replication forks that reverse after topoisomerase poisoning. EMBO Rep. *19*,

e45535. https://doi.org/10.15252/embr.201745535.

34. Cotta-Ramusino, C., Fachinetti, D., Lucca, C., Doksani, Y., Lopes, M., Sogo, J., and Foiani, M. (2005). Exo1 processes stalled replication forks and counteracts fork reversal in checkpoint-defective cells. Mol. Cell. *17*, 153–159. https://doi.org/10.1016/j.molcel.2004.11.032.

35. Segurado, M., and Diffley, J.F. (2008). Separate roles for the DNA damage checkpoint protein kinases in stabilizing DNA replication forks. Genes Dev. *22*, 1816–1827. https://doi.org/10.1101/gad.477208.

36. Larsen, N.B., Liberti, S.E., Vogel, I., Jørgensen, S.W., Hickson, I.D., and Mankouri, H.W. (2017). Stalled replication forks generate a distinct mutational signature in yeast. Proc. Natl. Acad. Sci. USA *114*, 9665–9670. https://doi.org/10.1073/pnas.1706640114.

37. Ghaddar, N., Corda, Y., Luciano, P., Galli, M., Doksani, Y., and Géli, V. (2023). The COMPASS subunit Spp1 protects nascent DNA at the Tus/Ter replication fork barrier by limiting DNA availability to nucleases. Nat. Commun. *14*, 5430. https://doi.org/10.1038/s41467-023-41100-4.

38. Tran, P.T., Erdeniz, N., Dudley, S., and Liskay, R.M. (2002). Characterization of nuclease-dependent functions of Exo1p in Saccharomyces cerevisiae. DNA Repair *1*, 895–912. https://doi.org/10.1016/s1568-7864(02)00114-3.

39. Gioia, M., Payero, L., Salim, S., Fajish, V.G., Farnaz, A.F., Pannafino, G., Chen, J.J., Ajith, V.P., Momoh, S., Scotland, M., et al. (2023). Exo1 protects DNA nicks from ligation to promote crossover formation during meiosis. PLoS Biol. *21*, e3002085. https://doi.org/10.1371/journal.pbio.3002085.

40. Schleicher, E.M., Dhoonmoon, A., Jackson, L.M., Khatib, J.B., Nicolae, C.M., and Moldovan, G.L. (2022). The TIP60-ATM axis regulates replication fork stability in BRCA-deficient cells. Oncogenesis *11*, 33. https://doi.org/10.1038/s41389-022-00410-w.

41. Kolinjivadi, A.M., Sannino, V., De Antoni, A., Zadorozhny, K., Kilkenny, M., Techer, H., Baldi, G., Shen, R., Ciccia, A., Pellegrini, L., et al. (2017). Smarcal1-mediated fork reversal triggers Mre11-dependent degradation of nascent DNA in the absence of Brca2 and stable Rad51 nucleofilaments. Mol. Cell. *67*, 867–881.e7. https://doi.org/10.1016/j.molcel.2017.07.001.

42. Taglialatela, A., Alvarez, S., Leuzzi, G., Sannino, V., Ranjha, L., Huang, J.W., Madubata, C., Anand, R., Levy, B., Rabadan, R., et al. (2017). Restoration of replication fork stability in BRCA1- and BRCA2-deficient cells by inactivation of SNF2-family fork remodelers. Mol. Cell. *68*, 414–430.e8. https://doi.org/10.1016/j.molcel.2017.09.036.

43. Vujanovic, M., Krietsch, J., Raso, M.C., Terraneo, N., Zellweger, R., Schmid, J.A., Taglialatela, A., Huang, J.W., Holland, C.L., Zwicky, K., et al. (2017). Replication fork slowing and reversal upon DNA damage require PCNA poly-ubiquitination and ZRANB3 DNA translocase activity. Mol. Cell. *67*, 882–890.e5. https://doi.org/10.1016/j.molcel.2017.08.010.

44. Puddu, F., Oelschlaegel, T., Guerini, I., Geisler, N.J., Niu, H., Herzog, M., Salguero, I., Ochoa-Montaño, B., Viré, E., Sung, P., et al. (2015). Synthetic viability genomic screening defines Sae2 function in DNA

repair. EMBO J. *34*, 1509–1522. https://doi.org/10.15252/embj.201590973.

45. Mallory, J.C., and Petes, T.D. (2000). Protein kinase activity of Tel1p and Mec1p, two Saccharomyces cerevisiae proteins related to the human ATM protein kinase. Proc. Natl. Acad. Sci. USA *97*, 13749–13754. https://doi.org/10.1073/pnas.250475697.

46. Lopes, M., Foiani, M., and Sogo, J.M. (2006). Multiple mechanisms control chromosome integrity after replication fork uncoupling and restart at irreparable UV lesions. Mol. Cell. *21*, 15–27. https://doi.org/10.1016/j.molcel.2005.11.015.

47. Yang, W. (2011). Surviving the sun: Repair and bypass of DNA UV lesions. Protein Sci. *20*, 1781–1789. https://doi.org/10.1002/pro.723.

48. Marians, K.J. (2018). Lesion Bypass and the Reactivation of Stalled Replication Forks. Annu. Rev. Biochem. *87*, 217–238. https://doi.org/10.1146/annurev-biochem-062917-011921.

49. Moore, C.W. (1989). Cleavage of Cellular and Extracellular Saccharomyces Cerevisiae DNA by Bleomycin and Phleomycin. Cancer Res. *49*, 6935–6940.

50. Sertic, S., Quadri, R., Lazzaro, F., and Muzi-Falconi, M. (2020). EXO1: A tightly regulated nuclease. DNA Repair *93*, 102929. https://doi.org/10.1016/j.dnarep.2020.102929.

51. Sokolsky, T., and Alani, E. (2000). EXO1 and MSH6 Are High-Copy Suppressors of Conditional Mutations in the MSH2 Mismatch Repair Gene of Saccharomyces cerevisiae. Genetics *155*, 589–599. https://doi.org/10.1093/genetics/155.2.589.

52. Greenwell, P.W., Kronmal, S.L., Porter, S.E., Gassenhuber, J., Obermaier, B., and Petes, T.D. (1995). TEL1, a gene involved in controlling telomere length in S. cerevisiae, is homologous to the human ataxia telangiectasia gene. Cell *82*, 823–829. https://doi.org/10.1016/0092-8674(95)90479-4.

53. Takata, H., Kanoh, Y., Gunge, N., Shirahige, K., and Matsuura, A. (2004). Reciprocal association of the budding yeast ATM-related proteins Tel1 and Mec1 with telomeres in vivo. Mol. Cell. *14*, 515–522. https://doi.org/10.1016/s1097-2765(04)00262-x.

54. Hirano, Y., Fukunaga, K., and Sugimoto, K. (2009). Rif1 and Rif2 Inhibit Localization of Tel1 to DNA Ends. Mol. Cell. *33*, 312–322. https://doi.org/10.1016/j.molcel.2008.12.027.

55. Oh, J., Lee, S.J., Rothstein, R., and Symington, L.S. (2018). Xrs2 and Tel1 Independently Contribute to MR-Mediated DNA Tethering and Replisome Stability. Cell Rep. *25*, 1681–1692.e4. https://doi.org/10.1016/j.celrep.2018.10.030.

56. Menin, L., Colombo, C.V., Maestrini, G., Longhese, M.P., and Clerici, M. (2019). Tel1/ATM signaling to the checkpoint contributes to replicative senescence in the absence of telomerase. Genetics *213*, 411–429. https://doi.org/10.1534/genetics.119.302391.

57. Bermejo, R., Doksani, Y., Capra, T., Katou, Y.M., Tanaka, H., Shirahige, K., and Foiani, M. (2007). Top1- and Top2-mediated topological transitions at replication forks ensure fork progression and stability and prevent DNA damage checkpoint activation. Genes Dev. *21*, 1921–1936. https://doi.org/10.1101/gad.432107.

58. Giannattasio, M., Follonier, C., Tourrière, H., Puddu, F., Lazzaro, F., Pasero, P., Lopes, M., Plevani, P., and Muzi-Falconi, M. (2010). Exo1 competes with repair synthesis, converts NER intermediates to long ssDNA gaps, and promotes checkpoint activation. Mol. Cell. 40, 50–62. https://doi.org/10.1016/j.molcel.2010.09.004.

59. Redon, C., Pilch, D.R., Rogakou, E.P., Orr, A.H., Lowndes, N.F., and Bonner, W.M. (2003). Yeast histone 2A serine 129 is essential for the efficient repair of checkpoint-blind DNA damage. EMBO Rep. 4, 678–684. https://doi.org/10.1038/sj.embor.embor871.

60. Goellner, E.M., Putnam, C.D., and Kolodner, R.D. (2015). Exonuclease 1-dependent and independent mismatch repair. DNA Repair 32, 24–32. https://doi.org/10.1016/j.dnarep.2015.04.010.

61. Calil, F.A., Li, B.Z., Torres, K.A., Nguyen, K., Bowen, N., Putnam, C.D., and Kolodner, R.D. (2021). Rad27 and Exo1 function in different excision pathways for mismatch repair in Saccharomyces cerevisiae. Nat. Commun. 12, 5568. https://doi.org/10.1038/s41467-021-25866-z.

62. Pichierri, P., Franchitto, A., Piergentili, R., Colussi, C., and Palitti, F. (2001). Hypersensitivity to camptothecin in MSH2 deficient cells is correlated with a role for MSH2 protein in recombinational repair. Carcinogenesis 22, 1781–1787. https://doi.org/10.1093/carcin/22.11.1781.

63. Jacob, S., Miquel, C., Sarasin, A., and Praz, F. (2005). Effects of camptothecin on double-strand break repair by non-homologous end-joining in DNA mismatch repair-deficient human colorectal cancer cell lines. Nucleic Acids Res. 33, 106–113. https://doi.org/10.1093/nar/gki154.

64. Gobbini, E., Cassani, C., Vertemara, J., Wang, W., Mambretti, F., Casari, E., Sung, P., Tisi, R., Zampella, G., and Longhese, M.P. (2018). The MRX complex regulates Exo1 resection activity by altering DNA end structure. EMBO J. 37, e98588. https://doi.org/10.15252/embj.201798588.

65. Lee, S.E., Moore, J.K., Holmes, A., Umezu, K., Kolodner, R.D., and Haber, J.E. (1998). Saccharomyces Ku70, mre11/rad50 and RPA Proteins Regulate Adaptation to G2/M Arrest after DNA Damage. Cell 94, 399–409. https://doi.org/10.1016/s0092-8674(00)81482-8.

66. Colombo, C.V., Menin, L., and Clerici, M. (2018). Alkaline Denaturing Southern Blot Analysis to Monitor Double-Strand Break Processing. Methods Mol. Biol. 1672, 131–145. https://doi.org/10.1007/978-1-4939-7306-4_11.

67. Ira, G., Malkova, A., Liberi, G., Foiani, M., and Haber, J.E. (2003). Srs2 and Sgs1-Top3 Suppress Crossovers during Double-Strand Break Repair in Yeast. Cell 115, 401–411. https://doi.org/10.1016/s0092-8674(03)00886-9.

68. Larsen, N.B., Sass, E., Suski, C., Mankouri, H.W., and Hickson, I.D. (2014). The Escherichia coli Tus-Ter replication fork barrier causes site-specific DNA replication perturbation in yeast. Nat. Commun. 5, 3574. https://doi.org/10.1038/ncomms4574.

69. Willis, N.A., Chandramouly, G., Huang, B., Kwok, A., Follonier, C., Deng, C., and Scully, R. (2014). BRCA1 controls homologous recombination at Tus/Ter-stalled mammalian replication forks. Nature 510, 556–559. https://doi.org/10.1038/nature13295.

70. Willis, N.A., Frock, R.L., Menghi, F., Duffey, E.E., Panday, A., Camacho, V., Hasty, E.P., Liu, E.T., Alt, F.W., and Scully, R. (2017). Mechanism of tandem duplication formation in BRCA1-mutant cells. Nature 551, 590–595. https://doi.org/10.1038/nature24477.

71. Marie, L., and Symington, L.S. (2022). Mechanism for inverted-repeat recombination induced by a replication fork barrier. Nat. Commun. 13, 32. https://doi.org/10.1038/s41467-021-27443-w.

72. Andersen, S.L., Sloan, R.S., Petes, T.D., and Jinks-Robertson, S. (2015). Genome-destabilizing effects associated with top1 loss or accumulation of top1 cleavage complexes in yeast. PLoS Genet. 11, e1005098. https://doi.org/10.1371/journal.pgen.1005098.

73. Pommier, Y., Sun, Y., Huang, S.N., and Nitiss, J.L. (2016). Roles of eukaryotic topoisomerases in transcription, replication and genomic stability. Nat. Rev. Mol. Cell Biol. 17, 703–721. https://doi.org/10.1038/nrm.2016.111.

74. Sloan, R., Huang, S.N., Pommier, Y., and Jinks-Robertson, S. (2017). Effects of camptothecin or TOP1 overexpression on genetic stability in Saccharomyces cerevisiae. DNA Repair 59, 69–75. https://doi.org/10.1016/j.dnarep.2017.09.004.

75. Sharma, K.G., Kaur, R., and Bachhawat, A.K. (2003). The glutathione-mediated detoxification pathway in yeast: An analysis using the red pigment that accumulates in certain adenine biosynthetic mutants of yeasts reveals the involvement of novel genes. Arch. Microbiol. 180, 108–117. https://doi.org/10.1007/s00203-003-0566-z.

76. Moreau, S., Ferguson, J.R., and Symington, L.S. (1999). The nuclease activity of Mre11 is required for meiosis but not for mating type switching, end joining, or telomere maintenance. Mol. Cell Biol. 19, 556–566. https://doi.org/10.1128/MCB.19.1.556.

77. Miyoshi, T., Kanoh, J., and Ishikawa, F. (2009). Fission yeast Ku protein is required for recovery from DNA replication stress. Gene Cell. 14, 1091–1103. https://doi.org/10.1111/j.1365-2443.2009.01337.x.

78. Sánchez, A., and Russell, P. (2015). Ku stabilizes replication forks in the absence of Brc1. PLoS One 10, e0126598. https://doi.org/10.1371/journal.pone.0126598.

79. Chanut, P., Britton, S., Coates, J., Jackson, S.P., and Calsou, P. (2016). Coordinated nuclease activities counteract Ku at single-ended DNA double-strand breaks. Nat. Commun. 7, 12889. https://doi.org/10.1038/ncomms12889.

80. Teixeira-Silva, A., Ait Saada, A., Hardy, J., Iraqui, I., Nocente, M.C., Fréon, K., and Lambert, S.A.E. (2017). The end-joining factor Ku acts in the end-resection of double strand break-free arrested replication forks. Nat. Commun. 8, 1982. https://doi.org/10.1038/s41467-017-02144-5.

81. Chen, B.R., Quinet, A., Byrum, A.K., Jackson, J., Berti, M., Thangavel, S., Bredemeyer, A.L., Hindi, I., Mosammaparast, N., Tyler, J.K., et al. (2019). XLF and H2AX function in series to promote replication fork stability. J. Cell Biol. 218, 2113–2123. https://doi.org/10.1083/jcb.201808134.

82. Garzón, J., Ursich, S., Lopes, M., Hiraga, S., and Donaldson, A.D. (2019). Human RIF1-Protein Phosphatase 1 Prevents Degradation and Breakage of Nascent DNA on Replication Stalling. Cell Rep. 27, 2558–2566.e4. https://doi.org/10.1016/j.celrep.2019.05.002.

83. Mukherjee, C., Tripathi, V., Manolika, E.M., Heijink, A.M., Ricci, G., Merzouk, S., de Boer, H.R., Demmers, J., van Vugt, M.A.T.M., and Ray Chaudhuri, A. (2019). RIF1 promotes replication fork protection and efficient restart to maintain genome stability. Nat. Commun. 10, 3287. https://doi.org/10.1038/s41467-019-11246-1.

84. Dhoonmoon, A., Nicolae, C.M., and Moldovan, G.L. (2022). The KU-PARP14 axis differentially regulates DNA resection at stalled replication forks by MRE11 and EXO1. Nat. Commun. 13, 5063. https://doi.org/10.1038/s41467-022-32756-5.

85. Audoynaud, C., Schirmeisen, K., Ait Saada, A., Gesnik, A., Fernández-Varela, P., Boucherit, V., Ropars, V., Chaudhuri, A., Fréon, K., Charbonnier, J.B., and Lambert, S.A.E. (2023). RNA:DNA hybrids from Okazaki fragments contribute to establish the Ku-mediated barrier to replication-fork degradation. Mol. Cell. 83, 1061–1074.e6. https://doi.org/10.1016/j.molcel.2023.02.008.

86. Porter, S.E., Greenwell, P.W., Ritchie, K.B., and Petes, T.D. (1996). The DNA-binding protein Hdf1p (a putative Ku homologue) is required for maintaining normal telomere length in Saccharomyces cerevisiae. Nucleic Acids Res. 24, 582–585. https://doi.org/10.1093/nar/24.4.582.

87. Balestrini, A., Ristic, D., Dionne, I., Liu, X.Z., Wyman, C., Wellinger, R.J., and Petrini, J.H. (2013). The Ku heterodimer and the metabolism of single-ended DNA double-strand breaks. Cell Rep. 3, 2033–2045. https://doi.org/10.1016/j.celrep.2013.05.026.

88. Ryan, A.J., Squires, S., Strutt, H.L., and Johnson, R.T. (1991). Camptothecin cytotoxicity in mammalian cells is associated with the induction of persistent double strand breaks in replicating DNA. Nucleic Acids Res. 19, 3295–3300. https://doi.org/10.1093/nar/19.12.3295.

89. Shiu, J.L., Wu, C.K., Chang, S.B., Sun, Y.J., Che, Y.J., Lai, C.C., Chiu, W.T., Chang, W.T., Myung, K., Su, W.P., and Liaw, H. (2020). The HLTF–PARP1 interaction in the progression and stability of damaged replication forks caused by methyl methanesulfonate. Oncogenesis 9, 104. https://doi.org/10.1038/s41389-020-00289-5.

90. Zellweger, R., Dalcher, D., Mutreja, K., Berti, M., Schmid, J.A., Herrador, R., Vindigni, A., and Lopes, M. (2015). Rad51-mediated replication fork reversal is a global response to genotoxic treatments in human cells. J. Cell Biol. 208, 563–579. https://doi.org/10.1083/jcb.201406099.

91. Ho, C.K., Mazón, G., Lam, A.F., and Symington, L.S. (2010). Mus81 and Yen1 promote reciprocal exchange during mitotic recombination to maintain genome integrity in budding yeast. Mol. Cell. 40, 988–1000. https://doi.org/10.1016/j.molcel.2010.11.016.

92. Matos, J., Blanco, M.G., Maslen, S., Skehel, J.M., and West, S.C. (2011). Regulatory control of the resolution of DNA recombination intermediates during meiosis and mitosis. Cell 147, 158–172. https://doi.org/10.1016/j.cell.2011.08.032.

93. Lee, B.I., and Wilson, D.M. (1999). The RAD2 domain of human exonuclease 1 exhibits 5'

to 3' exonuclease and flap structure-specific endonuclease activities. J. Biol. Chem. *274*, 37763–37769. https://doi.org/10.1074/jbc. 274.53.37763.

94. Beyer, T., and Weinert, T. (2016). Ontogeny of Unstable Chromosomes Generated by Telomere Error in Budding Yeast. PLoS Genet. *12*, e1006345. https://doi.org/10. 1371/journal.pgen.1006345.

95. Savitsky, K., Bar-Shira, A., Gilad, S., Rotman, G., Ziv, Y., Vanagaite, L., Tagle, D.A., Smith, S., Uziel, T., Sfez, S., et al. (1995). A single ataxia telangiectasia gene with a product similar to PI-3 kinase. Science *268*, 1749–1753. https://doi.org/10.1126/science. 7792600.

96. Wu, Y., Berends, M.J., Post, J.G., Mensink, R.G., Verlind, E., Van Der Sluis, T., Kempinga, C., Sijmons, R.H., van der Zee, A.G., Hollema, H., et al. (2001). Germline mutations of EXO1 gene in patients with hereditary nonpolyposis colorectal cancer (HNPCC) and atypical HNPCC forms. Gastroenterology *120*, 1580–1587. https:// doi.org/10.1053/gast.2001.25117.

97. García, M.E.G., Kirsch, D.G., and Reitman, Z.J. (2022). Targeting the ATM Kinase to Enhance the Efficacy of Radiotherapy and Outcomes for Cancer Patients. Semin. Radiat. Oncol. *32*, 3–14. https://doi.org/10. 1016/j.semradonc.2021.09.008.

98. Ueno, S., Sudo, T., and Hirasawa, A. (2022). ATM: Functions of ATM Kinase and Its Relevance to Hereditary Tumors. Int. J. Mol. Sci. *23*, 523. https://doi.org/10.3390/ ijms23010523.

99. van de Kooij, B., Schreuder, A., Pavani, R., Garzero, V., Uruci, S., Wendel, T.J., van Hoeck, A., San Martin Alonso, M., Everts, M., Koerse, D., et al. (2024). EXO1 protects BRCA1-deficient cells against toxic DNA lesions. Mol. Cell. *84*, 659–674.e7. https:// doi.org/10.1016/j.molcel.2023.12.039.

100. Tran, P.T., Erdeniz, N., Symington, L.S., and Liskay, R.M. (2004). EXO1-A multi-tasking eukaryotic nuclease. DNA Repair *3*, 1549–1559. https://doi.org/10.1016/j.dnarep. 2004.05.015.

101. Tran, P.T., Fey, J.P., Erdeniz, N., Gellon, L., Boiteux, S., and Liskay, R.M. (2007). A mutation in EXO1 defines separable roles in DNA mismatch repair and post-replication repair. DNA Repair *6*, 1572–1583. https:// doi.org/10.1016/j.dnarep.2007.05.004.

102. Trovesi, C., Falcettoni, M., Lucchini, G., Clerici, M., and Longhese, M.P. (2011). Distinct cdk1 requirements during single-strand annealing, noncrossover, and crossover recombination. PLoS Genet. *7*, e1002263. https://doi.org/10.1371/journal. pgen.1002263.

STAR★METHODS

KEY RESOURCES TABLE

REAGENT or RESOURCE	SOURCE	IDENTIFIER
Antibodies		
Anti-Rad53	Abcam	Cat#Ab104232; RRID: AB_2687603
Bacterial and virus strains		
Subcloning EfficiencyTM DH5alpha Competent Cells	Invitrogen	Cat#18265017
Chemicals, peptides, and recombinant proteins		
SspI-HF	NEB	Cat#R3132L
EcoRI-HF	NEB	Cat#R301L
Hygromycin B	Roche	Cat#10843555001
ClonNAT (nourseothricin)	Jena Bioscience	Cat#AB-102
G-418 disulfate	Merck	Cat#A1720
Phleomycin	Merck	Cat#P9564-100MG
(S)-(+)-Camptothecin	Merck	Cat#C9911-1G
Hydroxyurea	Merck	Cat#H8627-100G
Methyl methanesulfonate	Merck	Cat#129925
Zymolyase 20T	Nacalai Tesque	Cat#07663-91
EASYTIDES UTP [alpha-32P]	Perkin Elmer	Cat#NEG507T250UC
EASYTIDES dATP [alpha −32P]	Perkin Elmer	Cat#NEG512H250UC
D(+)-Raffinose pentahydrate	Merck	Cat#83400-100G
D(+)-Galactose	Merck	Cat#48260-500G-F
D(+)-Glucose monohydrate	Merck	Cat#49159-5KG
Yeast Extract Difco	BD	Cat#212750
Peptone Difco	BD	Cat#211677
Peptone Oxoid	OXOID	Cat#LP0037T
Yeast extract Oxoid	OXOID	Cat#LP0021T
Agar Bacto Difco	BD	Cat#214030
Agarose LE	EuroClone	Cat#EMR920500
TAE buffer (50X)	EuroClone	Cat#APA16911000
Methanol	Merck	Cat#179337-2.5L
Trichloroacetic acid	Merck	Cat#91230-1KG
RNase A	Roche	Cat#10109169001
Bromophenol Blue sodium salt	Merck	Cat#B6131-25G
tRNA	Roche	Cat#10109495001
Sodium Chloride	Merck	Cat#31434-M
Formamide	Merck	Cat#47671-1L-F
Denhardt's Solution 50x	Merck	Cat#D2532-5X5ML
Ficoll PM 400	Merck	Cat#F4375-25G
Triton X-100 for molecular biology	Merck	Cat#T8787-100ML
Dimethyl sulfoxide	Merck	Cat#D4540-1L
SSPE buffer 20X concentrate	Merck	Cat#S2015-1L
Deoxyribonucleic acid, single stranded from salmon testes	Merck	Cat#D7656-5X1ML
Yeast nitrogen base with amino acids	Merck	Cat#Y1250-250G
Hydrochloric acid	Merck	Cat#30721-1L-M

(Continued on next page)

Continued

REAGENT or RESOURCE	SOURCE	IDENTIFIER
Ethanol absolute	Merck	Cat#02860-2.5L
Ammonium persulfate	Merck	Cat#A3678-25G
N,N,N′,N′ -Tetramethylethylenediamine	Merck	Cat#T9281-50ML
Dextran sulfate sodium salt from *Leuconostoc* spp	Merck	Cat#D8906-100G
Acrylamide 4X solution	Serva	Cat#10677.1
N,N′-Methylene-bisacrylamide 2X	Serva	Cat#29197.01
2-Propanol	Merck	Cat#I9516-500ML
Glycine for electrophoresis, ≥99%	Merck	Cat#G8898-1KG
Sodium hydroxide	Merck	Cat#1064621000
Sodium dodecyl sulfate	Merck	Cat#L3771-500G
Trizma base	Merck	Cat#33742-2KG
Ponceau s sodium practical grade	Merck	Cat#P3504-100G
D-Sorbitol	Merck	Cat#S7547-1KG
Clarity Western ECL Substrate	Bio-Rad	Cat#1705061
2-Mercaptoethanol	Merck	Cat#97622
Nocodazole	Merck	Cat#1404-10MG
Sodium phosphate dibasic	Merck	Cat#S9763-1KG
Sodium phosphate monobasic	Merck	Cat#S3139-500G
Critical commercial assays		
Riboprobe System-T7	Promega	Cat#P1440
Invitrogen™ DECAprime™ II DNA Labeling Kit	Invitrogen	Cat#AM1455
QIAGEN QIAquick PCR Purification Kit	QIAGEN	Cat#28106
QIAquick Gel Extraction Kit	QIAGEN	Cat#28704
Experimental models: Organisms/strains		
Saccharomyces cerevisiae, see Table S4	This study	N/A
Oligonucleotides		
PRP 2969: CATAGCACACACCCACTTGC	Marie and Symington	N/A
PRP 2970: GAACAGTTGGTATATTAGGAGGG	Marie and Symington	N/A
PRP 2971: GTGGCAAGAATACCAAGAGTTCC	Marie and Symington	N/A
PRP 2972: GGACCAGAACTACCTGTG	Marie and Symington	N/A
Software and algorithms		
Scion Image Beta 4.0.2	Scion Corporation	N/A
OriginPro Lab	OriginLab Corporation	N/A
Other		
HYBOND-NX Nylon membrane	GE Healthcare	Cat#GEHRPN203T
Nitrocellulose blotting membrane, Amersham™ Protran™ 0.45 mm NC	GE Healthcare	Cat#GEH10600002
Hyperfilm MP	GE Healthcare	Cat#GEH28906844

RESOURCE AVAILABILITY

Lead contact

Further information and requests for resources and reagents should be directed to and will be fulfilled by the lead contact, Michela Clerici (michela.clerici@unimib.it).

Materials availability

All unique/stable reagents generated in this study are available from the lead contact without restriction.

Data and code availability

- All data reported in this paper will be shared by the lead contact upon request.
- This paper does not report original datasets or code.
- Any additional information required to reanalyze the data reported in this paper is available from the lead contact upon request.

EXPERIMENTAL MODEL AND STUDY PARTICIPANT DETAILS

All the strains used in this work are listed in Table S4 and are isogenic to W303, JKM139 and tGI354. Strains JKM139 and tGI354 used to detect DSB resection and DSB repair by ectopic recombination, respectively, were kindly provided by J. Haber (Brandeis University, Waltham, USA). The strain containing the *TerB* repeats in the blocking orientation at and the *TUS* gene under the control of the *GAL1* promoter[71] is derived from W303 and was kindly provided by L. Symington (Columbia University, New York, NY, USA). Gene deletions were carried out by one-step polymerase chain reaction (PCR) methods and standard yeast transformation methods. All genetic manipulations were verified by PCR.

The 2 μm plasmids carrying either the wild-type *EXO1* gene or the *exo1-D171A* allele[51] and the control vector was kindly provided by E. Alani (Cornell University, New York, NY, USA).

Cells were grown in YEP medium (1% yeast extract, 2% bacto-peptone) supplemented with 2% glucose (YEPD), 2% raffinose (YEPR) or 2% raffinose and 3% galactose (YEPRG). All experiments were performed at 26°C. CPT was dissolved in 2% DMSO before addition to the medium.

METHOD DETAILS

Spot assays and colony formation assay

Cells grown overnight were diluted to 1×10^7 cells/mL. 10-fold serial dilutions were spotted onto YEPD plates with or without DNA damaging agents, or before and after phleomycin treatment. Plates were incubated 25°C and pictures were taken after 3 days, except for HU-containing plates, which have been captured after 4 days at 25°C. For the colony formation assay, the number of colonies were determined after 3 days at 25°C and three technical duplicates from each strain were averaged.

Analysis of cell-cycle progression and western blotting

Exponentially growing cells were synchronized in the G1 phase of the cell cycle with 3 μg/mL α-factor. G1-arrested cells were then released into fresh YEPD medium with or without CPT at 10 μM. Cells were harvested, samples were analyzed to evaluate the budding index by optical microscopy and DNA was stained with propidium iodide to evaluate nuclear division by fluorescence microscopy. Protein extracts for western blotting were prepared following cell fixation with trichloroacetic acid (TCA) and were separated in 10% polyacrylamide gels, and then transferred to a nitrocellulose membrane.[33] Briefly, frozen cell pellets were resuspended in 100 μL 20% TCA. After the addition of acid-washed glass beads, the samples were vortexed for 10 min. The beads were washed with 400 μL of 5% TCA, and the extract was collected in a new tube. The crude extract was precipitated by centrifugation at 3000 rpm for 10 min. TCA was discarded, and samples were resuspended in 70 μL 2X Laemmli buffer (60 mM Tris, pH 6.8, 2% SDS, 10% glycerol, 100 mM DTT, 0.2% bromophenol blue) and 30 μL 1M Tris (pH 8.0). Samples were boiled at 99°C and centrifuged at 3000 rpm for 10 min. Supernatant containing the solubilized proteins were separated on 10% polyacrylamide gels. Rad53 was detected by using anti-Rad53 polyclonal antibodies (AB104232, Abcam) (1:2000).

Microcolony formation assay

Exponentially growing cells were synchronized in the G1 phase of the cell cycle with 3 μg/mL α-factor. G1-arrested cells were plated onto YEPD plates with CPT 10 μM dissolved in 1.2% DMSO.

Microcolony formation was assessed by counting cell bodies at optical microscope. G1-arrested cells were counted as one cell body, G2/M arrested cells (dumbbell shape cells) were counted as two cell bodies. Microcolonies contain more than two cell bodies. Microcolonies formation was scored until 8 h from G1-phase arrest.

Double-strand break end resection

YEPR exponentially growing cell cultures of JKM139 derivative strains, carrying the HO cut site at the *MAT* locus, were either synchronized in the G2 phase of the cell cycle with 5 μg/mL nocodazole for 2 h and transferred to YEPRG or directly transferred to YEPRG at time zero. SspI-digested genomic DNA was run on alkaline agarose gels and visualized after hybridization with a single-stranded RNA probe that anneals with the unresected strand at one side of the HO-induced DSB.[66] This probe was obtained by *in vitro* transcription using Promega Riboprobe System-T7 and plasmid pML514 as a template. Plasmid pML514 was constructed by inserting in the pGEM7Zf EcoRI site a 900-bp fragment containing part of the *MAT* locus (coordinates 200870 to 201587 on chromosome III). Quantitative analysis of DSB resection was performed by calculating the ratio of band intensities for ssDNA and the total amount of DSB products. The resection efficiency was normalized with respect to the HO cleavage efficiency for each time point. Densitometric analysis of band intensities was performed using Scion Image Beta 4.0.2 software.

Double-strand break repair by ectopic recombination

DSB repair by ectopic recombination was detected in tGI354 background. Briefly, YEPR exponentially growing cell cultures of tGI354 derivative strains were synchronized in the G2 phase of the cell cycle with 5 μg/mL nocodazole, and after 2 h cells were transferred to YEPRG. EcoRI-digested genomic DNA was run on agarose gels and visualized after hybridization with a DNA probe that anneals at the *MATa* locus.[102]

To determine the repair efficiency, the intensity of the uncut band at 2 h after HO induction (maximum efficiency of DSB formation) was subtracted from the normalized values of NCO and CO bands at the subsequent time points after galactose addition. The obtained values were divided by the normalized intensity of the uncut *MATa* band at time zero before HO induction (100%).

Densitometric analysis of band intensities was performed using Scion Image Beta 4.0.2 software.

Measurement of Ade+ recombination frequencies

To determine the percentage of Ade+ recombinants, strains were grown for 3 days on YEPD or 4 days on YEPG (1% yeast extract, 2% bacto-peptone, 2% galactose) plates. Colonies of similar size were suspended in 1 mL of water, serially diluted (10-fold) and plated onto YEPD or synthetic complete-adenine (SC-Ade) medium.[71]

Colonies were counted 2 days after plating and two dilutions from each initial colony were averaged. The percent Ade+ recombinants were determined by the ratio of the number of colonies growing on SC-Ade plates and YEPD plates × 100. Each data point in the graphs shows the percentage of Ade+ recombinants measured from one initial colony. Recombination frequencies were determined using the method of the median.

Distribution of Ade+ recombinants

Inversions and conversions were scored by PCR.[71] Primer PRP2969 that anneals to the *his2* sequence upstream of the *ade2* reporter was used together with primer PRP2972 that anneals to the *TRP1* sequence in the opposite orientation to detect inversions. PRP2972 was used together with PRP2970 that anneals to the *ade2-n* cassette to detect gene conversions events. The number of independent recombinants tested for each strain and condition, together with the number of inversions and conversions, is indicated in the Supplemental information. Primer sequences are reported in key resources table.

QUANTIFICATION AND STATISTICAL ANALYSIS

Statistical analysis

Data are expressed as mean values $\pm$ SD or SEM. quantification and statistical analysis were done using OriginLab Pro. *p*-values were calculated by two-tailed Student's t test.

Ade+ recombination frequencies were analyzed on log transformed values by one-way ANOVA with a Bonferroni post-test. Spontaneous and Tus/Ter associated data were analyzed separately. Distributions of inversions and conversions among Ade+ recombinants were analyzed by a two-tailed Chi-square test. Stars indicate a significant difference with the wild-type strain in the same condition: *p-value <0.05, **p-value <0.005, ***p-value <0.001, ****p-value <0.0001. Exact p-values are provided in the supplemental information file.